ORIGINAL ARTICLE

Modelling and parameter identification of coefficient of friction for deep-drawing quality steel sheets using the CatBoost machine learning algorithm and neural networks

Sherwan Mohammed Najm[1,2] · Tomasz Trzepieciński[3] · Marek Kowalik[4]

Abstract

The development of models for the coefficient of friction is difficult due to many factors influencing its value and many tribological phenomena that accompany contact between metals (i.e., flattening, ploughing, adhesion), the influence of which also depends on the friction conditions. Therefore, developing an analytical model of friction is difficult. In this article, the CatBoost machine learning algorithm, newly developed by Yandex researchers and engineers, is used for modelling and parameter identification of friction coefficients for three grades of deep-drawing quality steel sheets. Experimental tests to determine the friction coefficient were carried out using the strip drawing method with the use of a specially designed tribological device. Lubrication conditions, normal force, and the surface roughness of countersample surfaces were used as input parameters. The friction tests were conducted in dry friction and lubricated conditions with three grades of oils with a wide range of viscosities. Different transfer functions and various training algorithms were tested to build the optimal structure of the artificial neural networks. An analytical equation based on the parameters that were being investigated was created to calculate the COF of each material. Different methods of partitioning weight were employed for the expected COF to assess the relative importance (RI) and individual feature's relevance. A Shapley decision plot, which uses cumulative Shapley additive explanations (SHAP) values, was used to depict models for predicting COF. CatBoost was able to predict the coefficient of friction with R^2 values between 0.9547 and 0.9693 as an average for the training and testing dataset, depending on the grade of steel sheet. When considering all the materials that were tested, it was discovered that the Levenberg–Marquardt training algorithm performed the best in predicting the coefficient of friction.

Keywords Artificial neural networks · CatBoost · Coefficient of friction · Deep drawing · Friction · Sheet metal forming · Steel sheets

✉ Sherwan Mohammed Najm
 sherwan.mohammed@gpk.bme.hu

✉ Tomasz Trzepieciński
 tomtrz@prz.edu.pl

 Marek Kowalik
 m.kowalik@uthrad.pl

1 Department of Manufacturing Science and Engineering, Budapest University of Technology and Economics, Műegyetemrkp 3, 1111 Budapest, Hungary

2 Kirkuk Technical Institute, Northern Technical University, 36001 Kirkuk, Iraq

3 Department of Manufacturing Processes and Production Engineering, Rzeszow University of Technology, Al. Powst. Warszawy 8, 35-959 Rzeszów, Poland

4 Department of Machine Technology, Kazimierz Pulaski University of Technology and Humanities in Radom, 54 Stasieckiego Street, 26-600 Radom, Poland

1 Introduction

In the processes of sheet metal forming (SMF), the friction phenomenon is an inevitable phenomenon if there is metallic contact between two mating surfaces of the tool and the workpiece [1, 2]. Moreover, the phenomena related to friction, such as the ploughing of workpiece material by the surface asperities of the tool and adhesion and flattening of the surface asperities of the workpiece, change during the friction process [3]. In terms of surface roughness, the tool surface plays a key role because the hardness of the tool surface is greater than that of the deformed sheet [4, 5]. One of the effective methods of reducing friction in SMF is the use of lubricants of different consistencies (i.e., solid lubricants, fluids) and viscosities, as well as the use of special protective coatings that reduce the coefficient of friction (COF) [6, 7].
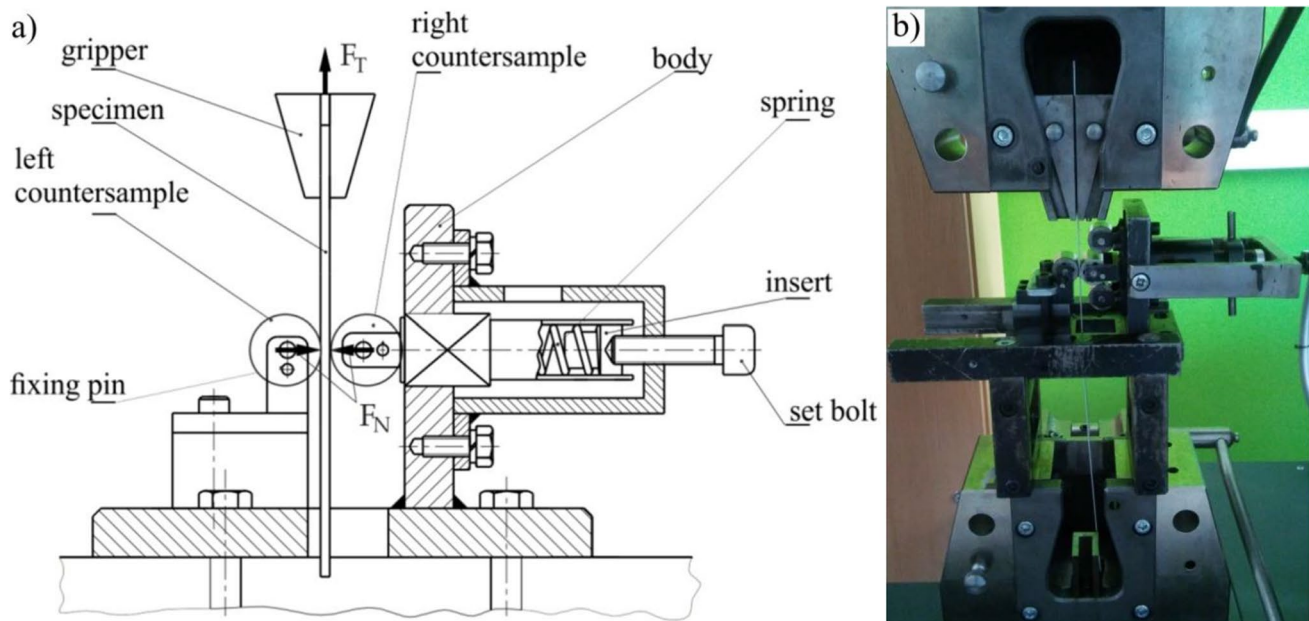
Fig. 1 **a** The layout and **b** photography of the friction testing device

Due to the complexity of the friction phenomenon depending on the friction conditions (dry friction, lubrication, normal pressure), process conditions (temperature, humidity, sliding speed), and surface properties (i.e., frictional anisotropy, surface roughness of the tool and workpiece, tool coating, tool material, tool and sheet material strength, tool hardness), developing a mathematical model based on analytical methods is extremely difficult [8–10].

The basic tool for stochastic data analysis is linear and multiple regression; however, due to the complexity of the description of the friction phenomenon, it is necessary to use multiple regression. The main goal of multiple regression is to quantify the relationship between multiple independent variables and the dependent variable [11]. Mathematical models based on statistical methods should have such a level
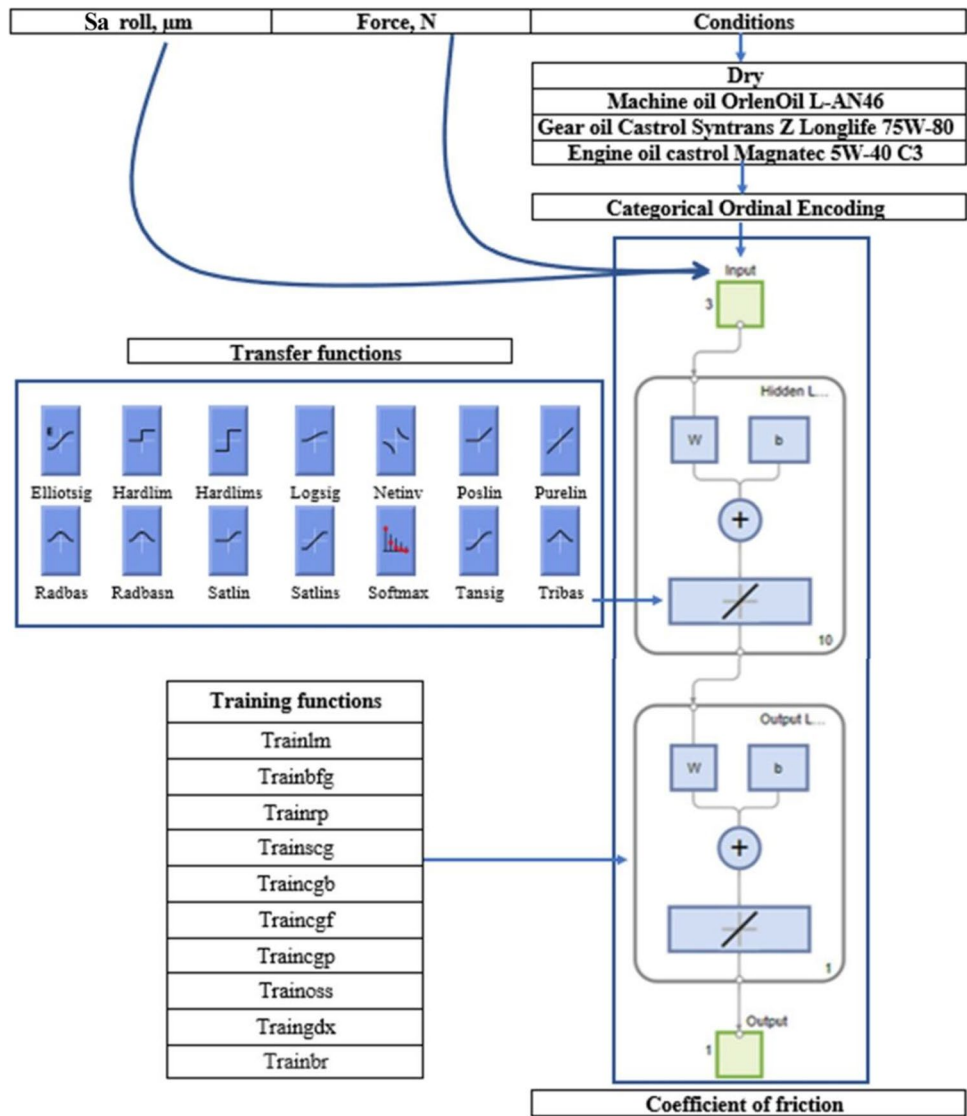
of complexity that they can reliably describe the phenomena occurring during the friction process [12, 13]. When selecting the factors affecting the COF, one should select those factors that significantly affect friction and are independent of each other at the same time. The condition of the significance of the influence of individual factors can be verified at a later stage of building the model, inter alia, by means of a posteriori elimination. The significance level is the assumed error probability when assessing the significance of the parameter. Usually, the significance level is set at $\alpha = 0.05$. Variance as the mean square deviation of the value of a random variable from its mean value is a measure of the dispersion of possible variable values and is an indispensable tool for testing the significance of the entire regression equation [14].

Within the wide application of regression analysis in tribology, particular attention should be paid to determining the value of the COF [15, 16] and to determining the effect of the load and the friction track on the wear rate [17]. The regression model proposed by Jurkovic et al. [18] took into account the influence of two factors, i.e., lubrication conditions and sheet deformation, on the value of the COF at the die edge. Experimental verification of the analytical model of friction in the draw bead that has been developed based on the multiple regression method has confirmed the possibility of using it to determine the resistance of the sheet passing through the draw bead in SMF [19]. Research on the frictional wear of materials used for vehicle brake pads has shown a very good applicability of the artificial neural network (ANN) method to regression, taking into account

Table 1 Experimental design

Parameter	Experimental parameters		
	Normal force, N	Average roughness of countersamples Sa, μm	Friction conditions
Volatility levels	31	0.44	Dry friction
	61	0.72	Machine oil
	92	1.57	L-AN46
	122	2.36	Gear oil
	152		SAE75W-80
	183		Engine oil
	213		SAE5W-40

Fig. 2 Multilayer perceptron structures

Sa roll, μm	Force, N	Conditions

| Dry |
| Machine oil OrlenOil L-AN46 |
| Gear oil Castrol Syntrans Z Longlife 75W-80 |
| Engine oil castrol Magnatec 5W-40 C3 |

Categorical Ordinal Encoding

Transfer functions

Elliotsig Hardlim Hardlims Logsig Netinv Poslin Purelin

Radbas Radbasn Satlin Satlins Softmax Tansig Tribas

Training functions
Trainlm
Trainbfg
Trainrp
Trainscg
Traincgb
Traincgf
Traincgp
Trainoss
Traingdx
Trainbr

Coefficient of friction

more than 20 input variables [20]. However, the number of explained variables in the model is not a determinant of its quality.

ANNs are a tool of soft computing that enables the construction of linear and nonlinear models which solve complex classification and regression tasks [21]. The structure of the network and the essence of the operation is a reflection of the biological brain. ANNs consist of a set of interconnected elements called neurons that process information delivered to the input of the network based on the idea of parallel processing. The architecture of the ANN includes, in addition to the input and output layers, one or more hidden layers. In most analyses, one hidden layer is sufficient to obtain satisfactory results [22]. As a result of the training process, ANNs can acquire the ability to predict output signals based on the sequence of input signals and the corresponding output signals. The analysis of the possibility of using ANNs in tribological studies was carried out by Grymek et al. [23],

pointing to the possibilities of using this technique in the analysis of tribological problems. According to the authors, the main error affecting the reduction of the quality of ANN predictions is the insufficient amount of training data used in the training process.

In the last two decades, the areas of successful incorporation of artificial intelligence generally and ANNs, in particular, have constantly been expanding in tribology research on brake performance [24, 25], wheel and rail wear [26], the surface roughness of extra deep drawing (EDD) steel [27], predicting of component hardness [28], surface roughness [29], and formability [30] in incremental sheet forming, friction in metal forming [31], and tool wear [32]. Increasing the accuracy of the ANN model was achieved by optimising the vector of explanatory variables with the use of genetic algorithms [31]. Rapetto et al. [33] studied the influence of surface roughness on real area of contact in rough contact by using a neural network. The ANN was able to prove the

Table 2 COF values determined at dry friction conditions

Sa of counter-samples, mm	Normal force, N	COF		
		Material B	Material SB	Material SSB
0.44	31	0.233	0.242	0.27
	61	0.228	0.234	0.273
	92	0.207	0.222	0.243
	122	0.216	0.215	0.234
	152	0.216	0.214	0.238
	183	0.201	0.210	0.234
	213	0.20	0.215	0.229
0.72	31	0.274	0.248	0.309
	61	0.257	0.241	0.29
	92	0.264	0.223	0.288
	122	0.241	0.226	0.266
	152	0.248	0.212	0.258
	183	0.235	0.206	0.244
	213	0.227	0.206	0.231
1.57	31	0.28	0.3	0.345
	61	0.282	0.282	0.324
	92	0.272	0.278	0.311
	122	0.257	0.265	0.301
	152	0.258	0.266	0.28
	183	0.24	0.274	0.276
	213	0.233	0.267	0.268
2.36	31	0.283	0.326	0.377
	61	0.274	0.326	0.358
	92	0.275	0.307	0.338
	122	0.273	0.294	0.336
	152	0.282	0.295	0.307
	183	0.279	0.281	0.31
	213	0.263	0.27	0.284

Table 3 COF values determined at machine oil L-AN46 lubrication

Sa of counter-samples, mm	Normal force, N	COF		
		Material B	Material SB	Material SSB
0.44	31	0.199	0.221	0.207
	61	0.191	0.222	0.209
	92	0.187	0.20	0.194
	122	0.182	0.199	0.198
	152	0.168	0.187	0.178
	183	0.164	0.184	0.169
	213	0.161	0.174	0.168
0.72	31	0.227	0.214	0.237
	61	0.23	0.20	0.232
	92	0.222	0.201	0.22
	122	0.22	0.188	0.214
	152	0.206	0.178	0.199
	183	0.206	0.176	0.201
	213	0.188	0.164	0.182
1.57	31	0.255	0.246	0.28
	61	0.244	0.22	0.258
	92	0.239	0.223	0.245
	122	0.228	0.204	0.244
	152	0.207	0.211	0.242
	183	0.212	0.195	0.234
	213	0.202	0.182	0.225
2.36	31	0.223	0.267	0.302
	61	0.229	0.27	0.305
	92	0.219	0.254	0.260
	122	0.206	0.255	0.249
	152	0.212	0.239	0.26
	183	0.195	0.243	0.225
	213	0.192	0.231	0.217

correlation between the roughness parameters and the real area of contact. A literature review on the use of ANNs in tribological applications was carried out by Frangu and Ripa [34]. The authors proved that ANNs are a useful tool during the design stage as well as the running stage. A review of computer techniques in modelling tribological effects is presented by Trzos [35]. As the review shows, the dissemination and wide use of scientific research in the area of tribology are limited due to the specific conditions of these processes but rather due to the lack of properly organised data storage systems that would enable a wider group of users to exchange data in the field of common research areas. Yin et al. [36] introduced the concept of tribo-informatics. In their paper, guided by the framework of tribo-informatics, they reviewed the application of tribo-informatic methods in tribology. ANNs, k-nearest neighbour, support vector machine, and random forest (RF) methods are those most commonly used by tribo-informatic practitioners. Bhaumik et al. [37] designed a new lubricant with multiple friction

modifiers using ANNs and a genetic algorithm which has been used for optimisation using the ANN models as the objective function. Experimental data generated by a pin-on-disc tribometer was used to train the ANNs. Pantić et al. [38] presented the possibility of applying ANNs to solve complex nonlinear problems and to identify the tribological characteristics of dental glass ceramics. An ANN model was used to describe the influence of input tribological parameters on COF and the rate of material wear. Gyurova and Friedrich [39] explored the potential for using ANNs for the prediction of the sliding friction properties of polyphenylene sulphide matrix composites based on the results of pin-on-disk sliding wear tests. It was found that the trained ANNs possessed enough capability to generalise to predict input data that were different from the original training dataset. The results of the research by Bhaumik and Kamaraj [40] showed that ANN and multi-criteria decision-making approaches can be used in the analysis of a blend of biodegradable lubricants in investigating its tribological properties and in reducing the

Table 4 COF values determined at gear oil SAE75W-80 lubrication

Sa of counter-samples, mm	Normal force, N	COF		
		Material B	Material SB	Materials SSB
0.44	31	0.167	0.202	0.19
	61	0.159	0.178	0.182
	92	0.164	0.184	0.169
	122	0.148	0.17	0.168
	152	0.154	0.166	0.167
	183	0.145	0.168	0.163
	213	0.142	0.15	0.15
0.72	31	0.199	0.181	0.199
	61	0.186	0.178	0.213
	92	0.18	0.181	0.196
	122	0.191	0.175	0.185
	152	0.173	0.167	0.189
	183	0.174	0.158	0.176
	213	0.173	0.152	0.178
1.57	31	0.193	0.219	0.255
	61	0.197	0.214	0.247
	92	0.184	0.202	0.232
	122	0.196	0.199	0.225
	152	0.187	0.198	0.213
	183	0.178	0.191	0.21
	213	0.185	0.181	0.193
2.36	31	0.205	0.252	0.24
	61	0.199	0.236	0.221
	92	0.176	0.235	0.22
	122	0.188	0.226	0.207
	152	0.168	0.227	0.18
	183	0.164	0.22	0.179
	213	0.164	0.218	0.18

Table 5 COF values determined at engine oil SAE5W-40 lubrication

Sa of counter-samples, mm	Normal force, N	COF		
		Material B	Material SB	Material SSB
0.44	31	0.169	0.164	0.166
	61	0.165	0.157	0.15
	92	0.147	0.158	0.152
	122	0.136	0.146	0.146
	152	0.132	0.148	0.149
	183	0.128	0.138	0.136
	213	0.131	0.139	0.131
0.72	31	0.174	0.187	0.164
	61	0.172	0.164	0.162
	92	0.166	0.162	0.157
	122	0.156	0.145	0.154
	152	0.158	0.142	0.141
	183	0.145	0.143	0.148
	213	0.145	0.14	0.137
1.57	31	0.21	0.186	0.228
	61	0.207	0.19	0.214
	92	0.175	0.173	0.219
	122	0.171	0.173	0.214
	152	0.172	0.16	0.19
	183	0.166	0.157	0.166
	213	0.158	0.136	0.17
2.36	31	0.185	0.26	0.252
	61	0.183	0.244	0.232
	92	0.185	0.228	0.226
	122	0.164	0.228	0.209
	152	0.166	0.22	0.186
	183	0.153	0.21	0.191
	213	0.147	0.191	0.171

number of experiments required to design the desired lubricant. Nasir et al. [41] applied a multilayer perceptron (MLP) to predict the COF of a glass fibre–reinforced thermosetting polyester. It was found that the tan-sigmoid transfer function exhibited the best performance for the work currently being carried out. Otero et al. [42] tested several different ANNs for predicting the lubricated friction coefficient in thermal-elastohydrodynamic contacts. It was concluded that properly trained MLPs are able to give an excellent prediction with a high level of correlation between calculations and experimental data. A perspective of the use of artificial intelligence in tribology has been provided by Rosenkranz et al. [43]. Analysis of the literature showed that ANNs and techniques that combined statistics and machine learning are suitable for highly complex, nonlinear applied problems, which makes them particularly interesting for various fields of tribology. Artificial intelligence and machine learning, which is a sub-domain of computer science, provide opportunities to explore the complex processes in tribological systems and to classify their behaviour in an efficient or even real-time way [43, 44]. Examples of the application of ANNs in tribological studies were presented, and important features of the data-driven modelling paradigm were discussed by Argatov [45].

The condition of a weak correlation of explanatory variables with each other is particularly important when building regression models. However, in the case of neural models, correlating the variables with each other has a much smaller negative impact on the quality of the model due to the natural ability of ANNs to weaken the influence of some inputs by minimising the weighting factors of neurons. The above-detailed issues, as well as the lack of well-defined requirements of the deep drawing COF and the absence of referent predictional mathematical models, have motivated the authors to examine the investigation and prediction of the COF. This article uses the CatBoost machine learning algorithm

Fig. 3 Training parameters
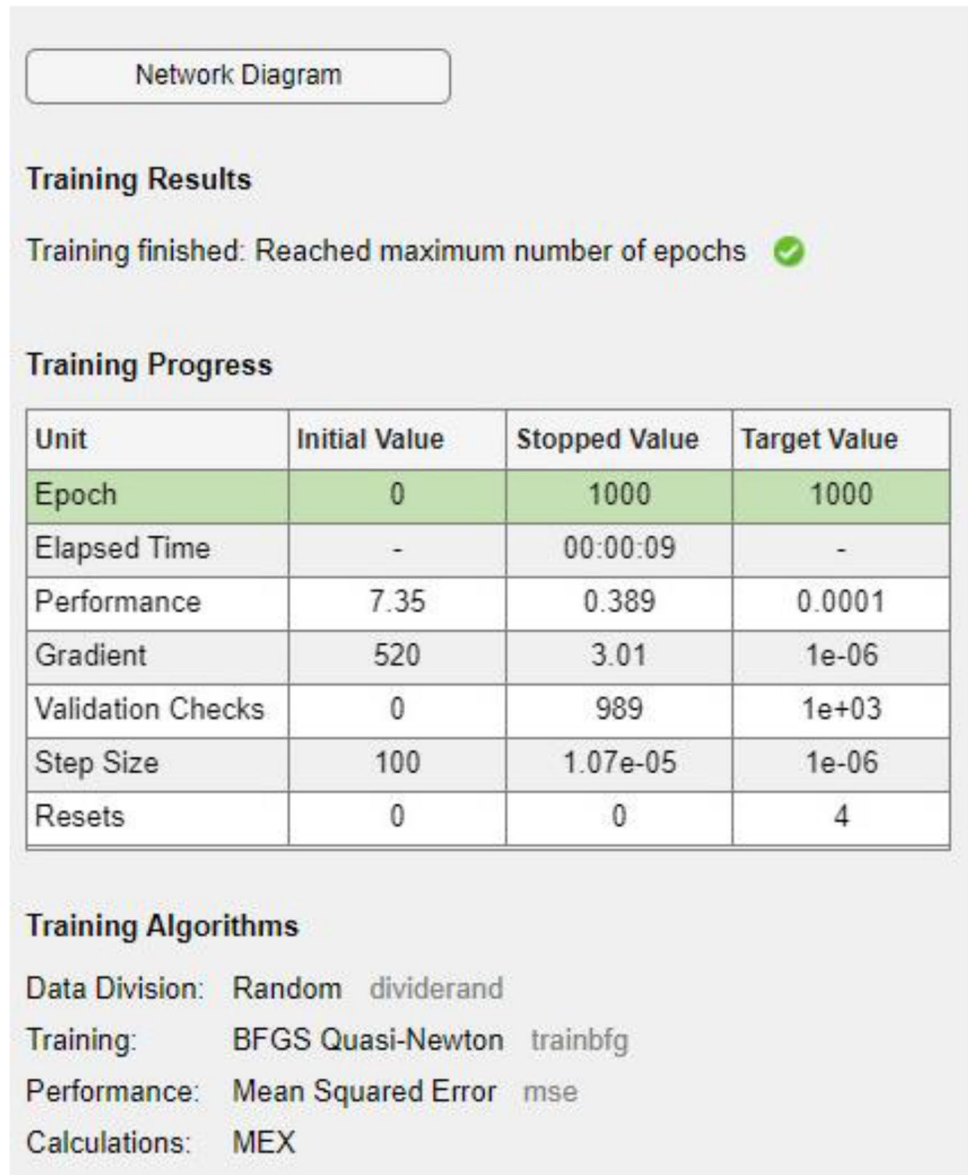
newly developed by Yandex researchers and engineers as an open-source library for gradient boosting on decision trees. Furthermore, multilayer perceptron (MLP) structures were developed to predict COF values. The effectiveness of this algorithm was verified on the basis of predictive models of the COF of three grades of

Table 6 Details of training functions used in multilayer perceptron

Algorithm	Acronym	Long term
Trainlm	LM	Levenberg–Marquardt
Trainbfg	BFG	BFGS quasi-Newton
Trainrp	RP	Resilient backpropagation
Trainscg	SCG	Scaled conjugate gradient
Traincgb	CGB	Conjugate gradient with Powell-Beale restarts
Traincgf	CGF	Conjugate gradient with Fletcher-Reeves updates
Traincgp	CGP	Conjugate gradient with Polak-Ribiére updates
Trainoss	OSS	OnOne step secant
Traingdx	GDX	Gradient descent with momentum and adaptive learning rate
Trainbr	BRB	Bayesian regularisation backpropagation

Table 7 Details of transfer functions used in multilayer perceptron

Acronym	Long term	Equations
Elliotsig	Elliot sigmoid	$f(x) = elliotsig(x) = (x)/1 + |x|$
Hardlim	Positive hard limit	$f(x) = hardlim(x) = 1$, if $x >= 0$; $= 0$, otherwise
Hardlims	Symmetric hard limit	$f(x) = hardlim(x) = 1$, if $x >= 0$; $= -1$, otherwise
Logsig	Logarithmic sigmoid	$f(x) = logsig(x) = 1 / (1 + exp(-x))$
Netinv	Inverse	$f(x) = netinv(x) = 1/x$
Poslin	Positive linear	$f(x) = poslin(x) = x$, if $x >= 0$; $= 0$, if $x <= 0$
Purelin	Linear	$f(x) = purelin(x) = x$
Radbas	Radial basis	$f(x) = radbas(x) = exp(-x^2)$
Radbasn	Radial basis normalised	$f(x) = radbasn(x) = exp(-x^2) / sum(exp(-x^2))$
Satlin	Positive saturating linear	$f(x) = satlin(x) = 0$, if $x <= 0$; $= x$, if $0 <= x <= 1$; $= 1$, if $1 <= x$
Satlins	Symmetric saturating linear	$f(x) = satlins(x) = -1$, if $x <= -1$; $= x$, if $-1 <= x <= 1$; $= 1$, if $1 <= x$
Softmax	Soft max	$f(x) = softmax(x) = exp(x)/sum(exp(x))$
Tansig	Symmetric sigmoid	$f(x) = tansig(x) = 2/(1 + exp(-2*x)) - 1$
Tribas	Triangular basis	$f(x) = tribas(x) = 1 - abs(x)$, if $-1 <= x <= 1$; $= 0$, otherwise

x is the weighted sum of w_i, b, and y of Eq. (2)

deep-drawing quality steel sheets. The most important parameters of the friction process, i.e., the surface roughness of countersamples, normal force value, and lubrication conditions, were selected as input variables. Instead of constructing, running, and evaluating a new ANN model each time, analytical equations for the prediction of COF values were retrieved from the best model. As a result, a new method was developed; one of the novelties and emerging findings of this research is to develop a neural network structure based on training and transfer functions with different conditions to extract the equation that predicts the COF from the best model that was implemented for the three different conditions. To the authors' knowledge, such an experimental process and predictions have not been tested or described in the literature. Furthermore, as an aim and novelty in the scope of this paper, a joint partitioning weight of the neural network was adopted to assess the relative importance (RI) of COF parameters on the output. According to the review work by Marian and Tremmel [44], the current showstopper in ANN modelling is still the lack of availability of sufficient and comparable datasets as well as the handling of uncertainties regarding test conditions and deviations. So, in this respect, the underlying databases and the corresponding models have been presented in appendices.

2 Materials and methods

2.1 Materials

Deep-drawing quality steel sheets commonly used in the automotive industry were used as test materials. According to PN-87/H-92143 [46], the drawability categories of these sheets are as follows:

– B (very deep drawing sheets),
– SB (sheets for very difficult drawpieces),
– SSB (sheets for particularly difficult drawpieces).

According to the international standard EN 10,130:2009 [47], the drawability categories B, SB, and SSB are equivalents of the drawability of the sheets DC03, DC04, and DC05, respectively.

2.2 Experimental setup

A specially designed tester (Fig. 1) mounted in a typical uniaxial tensile testing machine was used to carry out the strip drawing test. This test is commonly used to modelling the friction conditions in the flange area of drawpiece in the sheet metal forming. The body of the device is mounted in the lower holder of the testing machine. The upper end of a strip specimen was
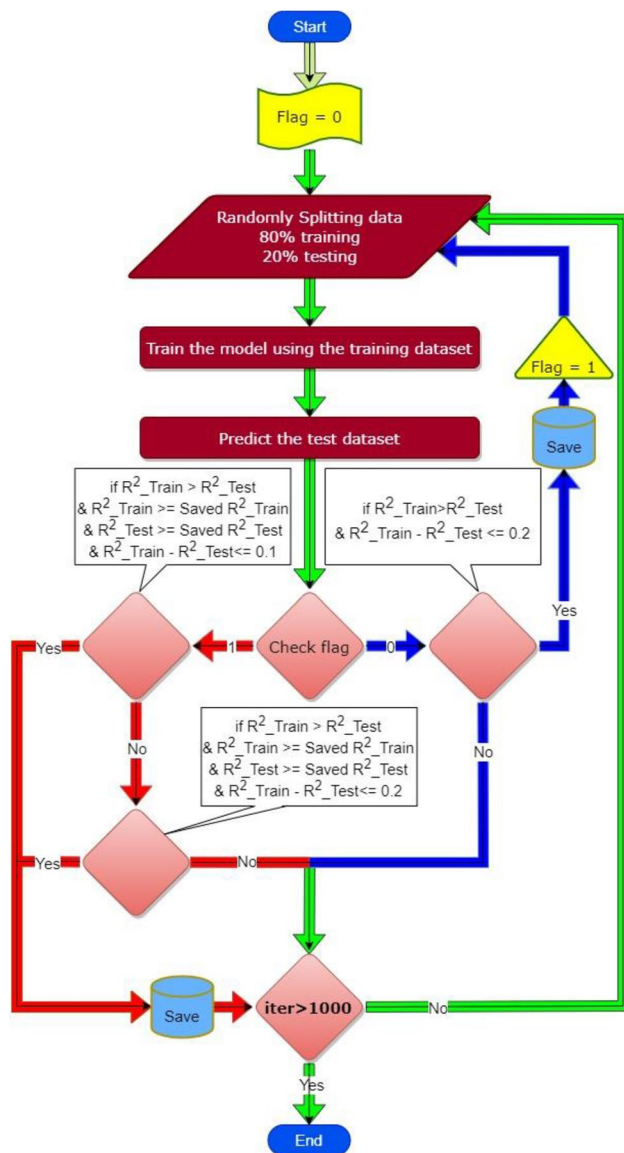
Fig. 4 Flowchart of the MLP model that was developed

mounted in the upper holder of the testing machine, crimped between two countersamples. Cylindrical countersamples with a radius of 20 mm were made of 145Cr6 cold-work tool steel. The countersamples were locked with fixing pins to prevent rotation. The left countersample was attached non-movably to the body of the testing device, while the right countersample was attached to a horizontal sleeve which could move horizontally in the body of the device. During the test, the lower holder of the uniaxial tensile testing machine with the mounted friction device did not move. Only the upper holder of the testing machine could move, causing the sheet metal strip to be pulled. Specimens for the friction test, approximately 200-mm long and 20-mm wide, were cut from the sheet metals along their rolling direction.

Normal force (thrust force) F_N was set by means of a spring, the working length of which was changed using

a set screw. The normal force value was changed in the range of 30–210 N with an increment of 30 N. The tangential force (friction force) F_T was recorded by the measuring system of a uniaxial tensile testing machine. Both forces were acquired with the same frequency. After correlating the force values in the Excel program, the average values of COF were determined using the formula:

$$\mu = \frac{F_T}{2F_N} \tag{1}$$

Four sets of countersamples with surface roughness Sa = 0.44 μm, Sa = 0.72 μm, Sa = 1.57 μm, and Sa = 2.36 μm were used in the tests. Contrary to the roughness of the countersamples, the sheets were selected in such a way that their surface roughness was similar, allowing for independent checking of the COF results for the sheets with varying drawability properties. The average surface roughness of the sheets Sa is equal to Sa = 1.46 μm (for B sheet), 1.38 μm (SB), and 1.29 μm (SSB). The COF values determined in the strip drawing test varied between about 0.12 and 0.38, depending on the friction conditions. However, these values are only valid in the flange area of the workpiece. Therefore, the strip drawing test is commonly used to model the friction conditions in the flange area of the drawpiece in the sheet metal forming.

The purpose of using countersamples with such roughnesses was to provide training data with a wide range of variability for training neural networks. The friction tests were carried out under conditions of dry friction and with lubrication of the sheet surface with typical oils used in the metal forming industry [48, 49]: machine oil L-AN46 (Orlen Oil), gear oil Systrans Z Longlife SAE75W-80 (Castrol), and Magnatec engine oil SAE5W-40. The viscosities of the oils provided by the manufacturers were as follows: gear oil SAE75W-85—55 mm²/s, machine oil LAN-46—43.9 mm²/s, and engine oil SAE5W-40 C3—81 mm²/s. Before starting the tests, the surfaces of the samples and countersamples were degreased with acetone. In the tests performed under lubrication conditions, a layer of machine oil was applied to the sample on both sides. The lubricant was distributed uniformly on the surface of the samples at 2 g/m² [50]. The sample was pulled through the countersample system with a constant top handle speed of 5 mm/s. Experimental matrix of friction tests is shown in Table 1.

2.3 CatBoost machine learning algorithm

CatBoost [51] is a high-performance open-source software for boosting the decision tree gradient. Yandex researchers and engineers created the CatBoost machine learning algorithm which incorporates numerous features. One of the key characteristics is the ability to use categorical data (non-numeric components) without the
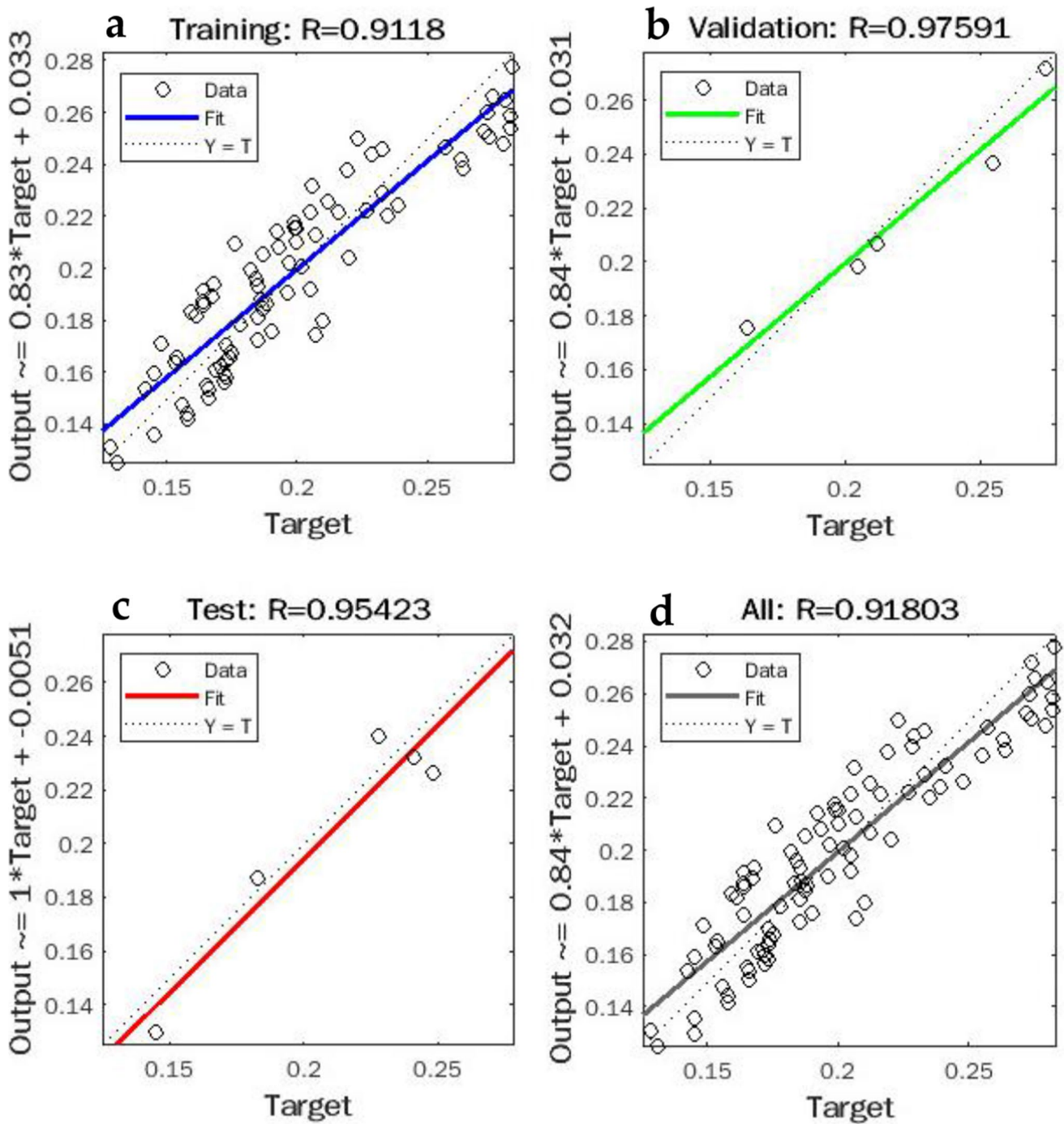
Fig. 5 Linear regression between the targets and outputs for sets: **a** training, **b** validation, **c** testing, and **d** all sets

need for pre-processing. In addition, converting such data to integers via encoding is not required [52].

On top of this, CatBoost makes accurate predictions with default values, eliminating the need to modify parameters [53]. CatBoost creates 1000 trees by default, fully symmetrical binary trees with six in-depth, and two leaves. The learning rate is calculated automatically based on the training dataset's attributes and the number of iterations. The learning rate chosen automatically should be close to ideal. For faster training, the number of iterations can be reduced, but the learning rate must be increased.

2.4 Multilayer perceptron

Net topology is the arrangement or structure of network elements and their connections, inputs, and outputs. The

Fig. 6 Neural network training performance
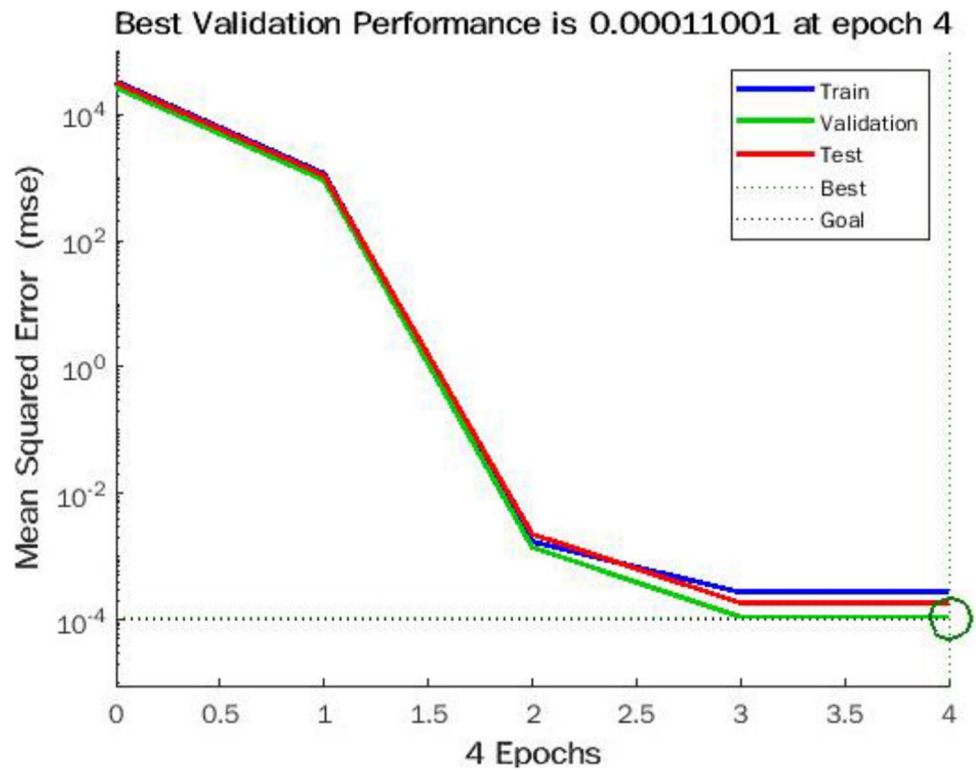
number of input and output layers and the transfer functions between these levels and the number of neurons in each layer can be used to describe the topology of an ANN [54]. The input and output layers of an ANN are separated by at least one hidden layer. Several neurons are present in each layer of the net. The number of input variables equals the number of input neurons, and the number of outputs associated with each input equals the number of output neurons. These neurons in the layers allow for the backward and forward transfer of weight between the layers based on the transfer function or the so-called activation function [55]. The current study uses a backpropagation learning approach. Werbos proposed the MLP idea in 1974, and Rumelhart,

McClelland, and Hinton proposed it in 1986 [56]. The multilayer perceptron is defined as follows in Eq. (2):

$$y = f(net) = f\left(\sum_{i=1}^{n} w_i x + b \right) \tag{2}$$

where y is the output and x is input, w_i are the weights, and b is the bias [57].

MLP structures were developed using MATLAB R2022a [58] to predict COF values. According to the purpose of this study, each net structure had one hidden layer with ten neurons connecting to the input and output layers, as shown in Fig. 2. Inputs have been obtained and target datasets using

Table 8 Validation metrics for checking CatBoost methods used for predicting the COF for material B

Validation metrics	Training	Testing	Training and testing
ME	− 0.0022	− 0.0008	− 0.0020
MAE	0.0056	0.0083	0.0061
MSE	0.0001	0.0001	0.0001
RMSE	0.0074	0.0098	0.0080
MRE	0.0292	0.0407	0.0315
SD	0.0071	0.0100	0.0078
SEM	0.0008	0.0021	0.0007
R^2	0.9668	0.9281	0.9602
adj. R^2	0.9682	0.9360	0.9621

Table 9 Validation metrics for checking CatBoost methods used for predicting the COF for material SB

Validation metrics	Training	Testing	Training and testing
ME	0.0013	− 0.0042	0.0002
MAE	0.0051	0.0114	0.0064
MSE	0.0001	0.0002	0.0001
RMSE	0.0073	0.0147	0.0093
MRE	0.0275	0.0528	0.0327
SD	0.0072	0.0144	0.0094
SEM	0.0008	0.0030	0.0009
R^2	0.9722	0.8818	0.9547
adj. R^2	0.9699	0.8426	0.9485

Table 10 Validation metrics for checking CatBoost methods used for predicting the COF for material SSB

Validation metrics	Training	Testing	Training and testing
ME	− 0.0007	− 0.0047	− 0.0015
MAE	0.0062	0.0092	0.0068
MSE	0.0001	0.0002	0.0001
RMSE	0.0082	0.0132	0.0094
MRE	0.0298	0.0412	0.0321
SD	0.0082	0.0126	0.0093
SEM	0.0009	0.0026	0.0009
R^2	0.9774	0.9324	0.9693
adj. R^2	0.9768	0.9224	0.9674

actual measured data from the experiments of three different materials have been adopted. The inputs have three neurons: Ra_roll (μm), force (N), friction conditions: dry and using oil, the COF values are the outputs. In the range of conditions using oil, three different oils have been selected: OrlenOil L-AN46 machine oil, Castrol Syntrans Z Longlife SAE75W-80 gear oil, and Castrol Magnatec SAE5W-40 C3 engine oil. The values of COF for all analysed friction cnditions are listed in Tables 2, 3, 4, and 5.

The other important parameters used for training in this study are a learning rate of 0.01, a performance target of 0.0001, and 1000 epochs, as shown in Fig. 3. Different training and transfer functions (see Tables 6 and 7) were tried and trained to identify the optimal model.

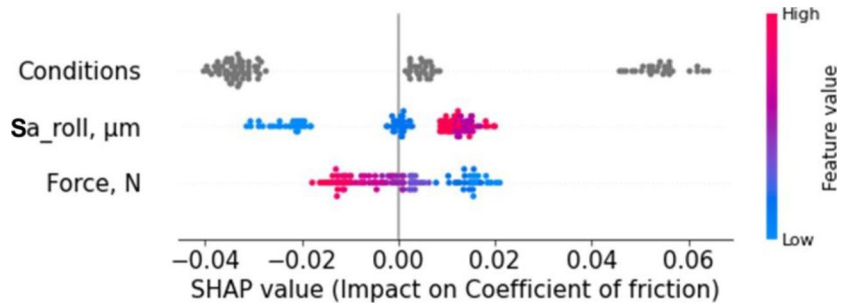**Fig. 7** Summary plot of SHAP value impact on COF for material B

Fig. 8 Summary plot of SHAP value impact on COF for material SB
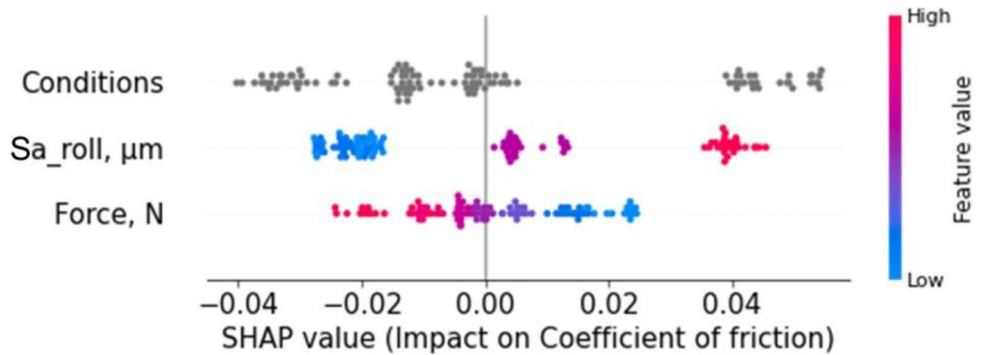
Fig. 9 Summary plot of SHAP value impact on COF for material SSB
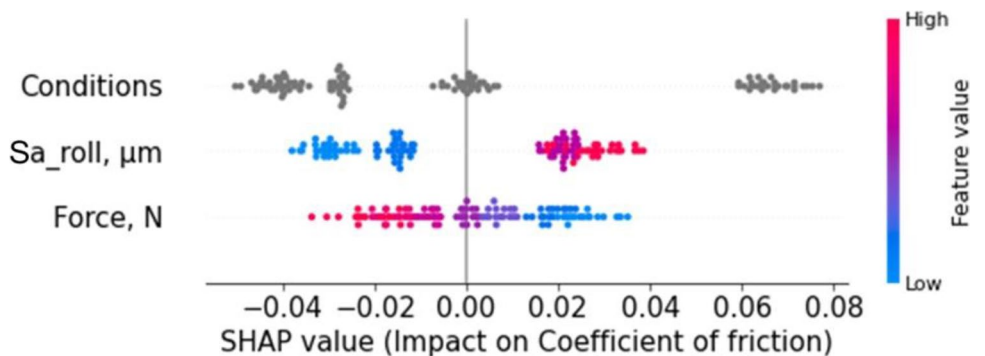
Fig. 10 SHAP decision plot for all prediction values of COF for material B
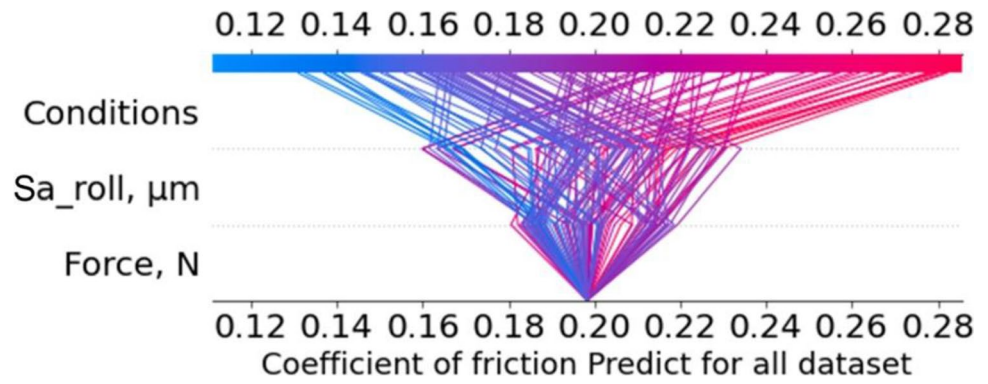
Fig. 11 SHAP decision plot for all prediction values of COF for material SB
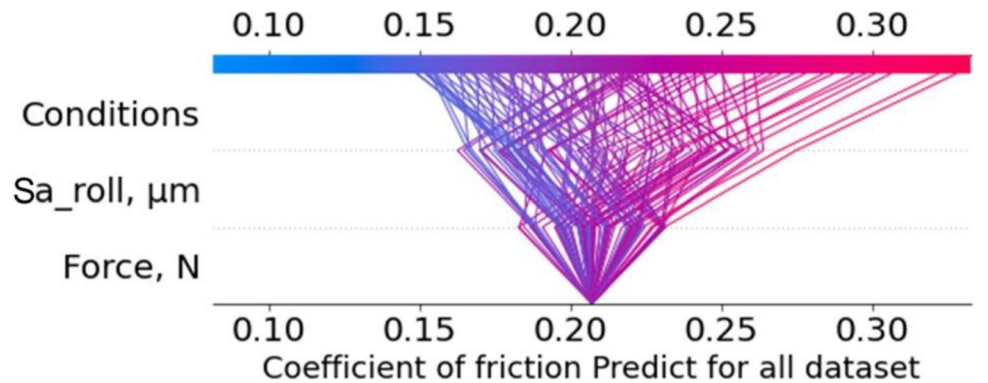
Figure 4 depicts the training flowchart in the model that was generated and the testing procedure utilising test data. During the running process, three primary conditions make decisions. The model and any variables with low condition limits are saved in the first loop, which is blue. After the first condition occurs, the second red loop is activated and stops. The second loop locates the training and variables, compares them to variables saved from prior training, and repeats the process until 1000 iterations have been completed. Green arrows indicate shared step loops.

The optimisation strategy is used in neural networks to tune and identify a set of network weights for constructing a suitable prediction map. Various optimisation algorithms, often known as training functions, exist. The training function is an algorithm for teaching the network to recognise and map a particular input to a specific output. Many factors influence the training function, including the trained dataset, weights, and biases, and the performance target. Selecting a suitable training function for the network is one problem in building good, rapid, and genuinely accurate predictions. Keeping this in mind, ten distinct forms of learning algorithms were used to map outputs to inputs in current MLP nets in the scope of this work. Table 6 lists the associated training functions.

The sums of each node are weighted in machine learning, and the accumulated weights are processed through an activation function "transfer function," which computes the output of each layer by using the summed weights that

Fig. 12 SHAP decision plot for all prediction values of COF for material SSB
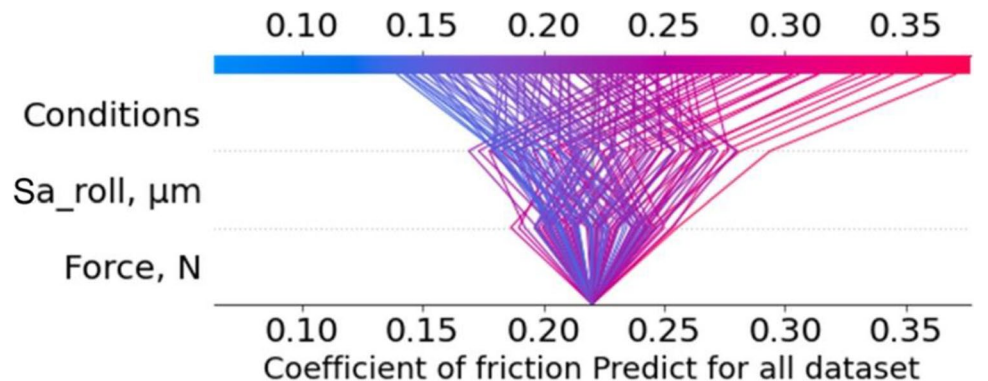
Fig. 13 Positive SHAP values: **a** SHAP decision plot and **b** SHAP bar plot

(a)

(b)
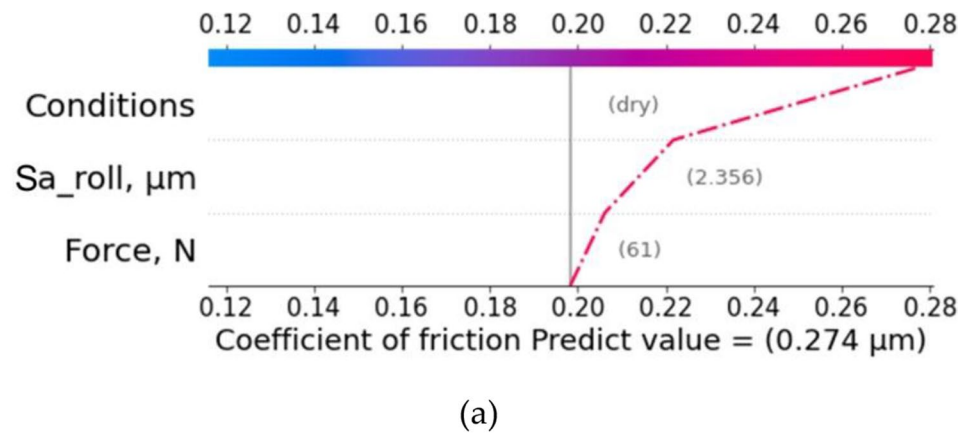
enter that layer. Setting correct transfer functions is a difficult undertaking that depends on various elements, the most important of which is network structure. There are many functions that are commonly used for pattern recognition; different transfer functions were used to increase prediction accuracy in this study. Table 7 summarises all the transfer function algorithms employed in this work, along with their corresponding equations.

The structures and models constructed and trained as part of this study to produce COF values as network

Fig. 14 Negative SHAP values: **a** SHAP decision plot and **b** SHAP bar plot

(a)

(b)
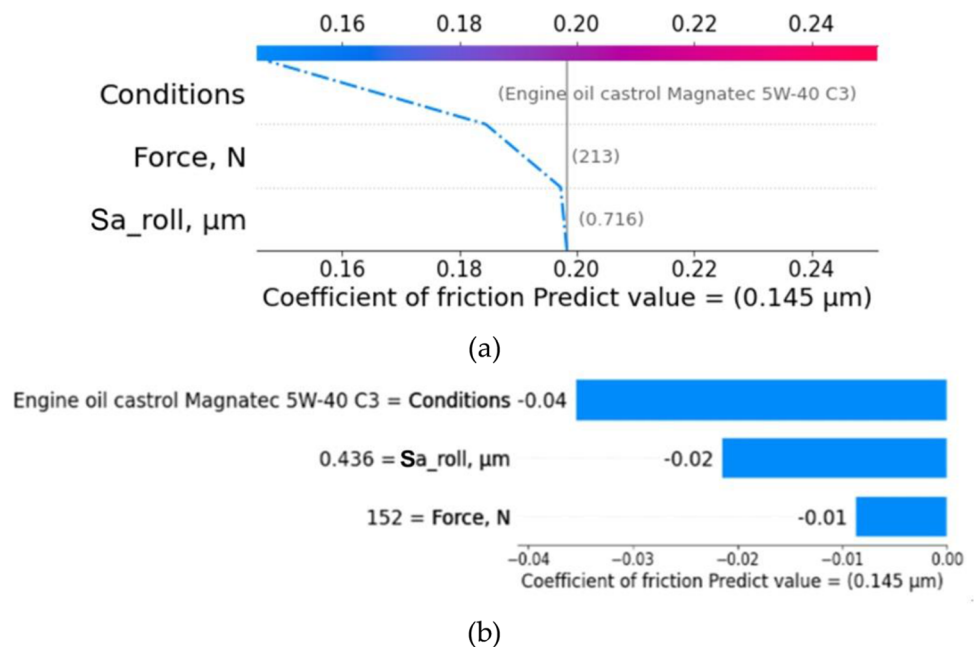
Fig. 15 Positive and negative SHAP values: **a** SHAP decision plot and **b** SHAP bar plot

(a)

(b)
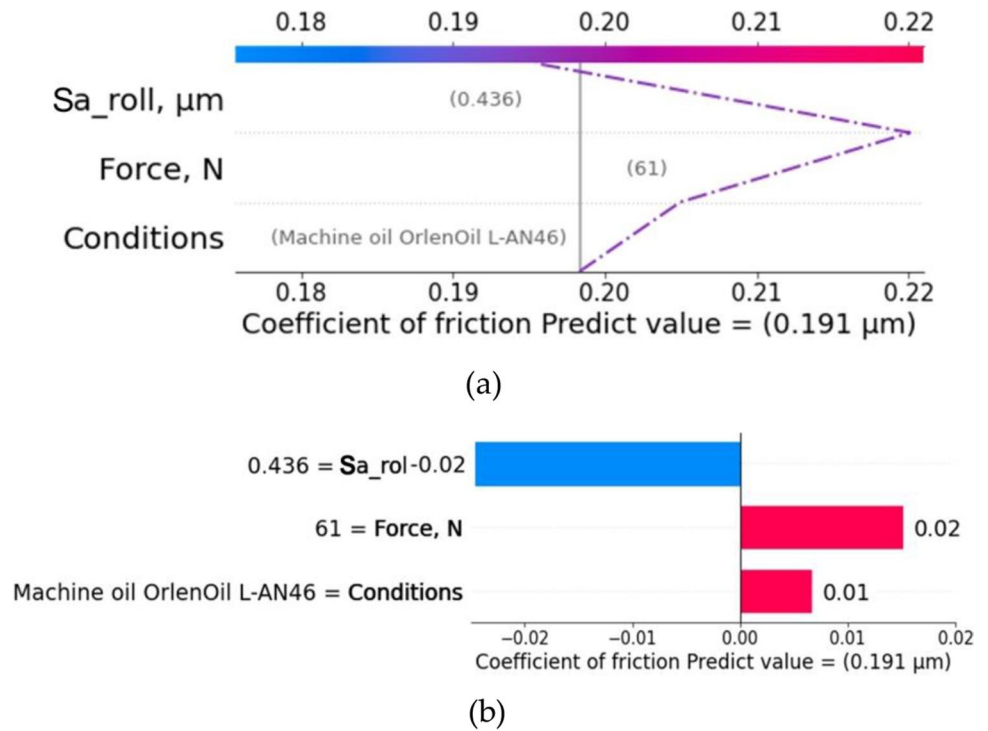
outputs used actual experimental values as input data. Data must be split into different subsets, such as training, validation, and testing datasets. In fact, splitting the dataset into training and testing subsets considerably impacts prediction accuracy and training performance [59]. Incorrect subgroups have a negative impact on benchmark performance. Shahin [60] asserted that the splitting ratio of the dataset has no obvious relationship, while Zhang et al. [59] said that it is one of the significant issues. As of now, there is no general solution accessible. Most researchers divided the datasets into lines with varying ratios

of subgroups based on their surveys. The most widely used ratios for teaching and assessment are 90 to 10%, 80 to 20%, or 70 to 30%. The optimal prediction was produced as part of a training run implemented for this paper which divided the actual data (112 samples) by 80% vs. 20% related to the input data. The data were randomly divided into training and testing sets; the training dataset was partitioned into validation and test subsets to ensure the model learned all data samples. Ninety percent of the training dataset was used for training, 5% for validation, and 5% for testing. The final testing dataset (20%)

Table 11 Validation metrics of the best multilayer perceptron (MLP) models for predicting COF (materials B, SB, and SSB)

Material	Material B		Material SB		Material SSB	
Training function	Levenberg–Marquardt (LM)—Trainlm					
Transfer function	Positive saturating linear—Satlin		Radial basis—Radbas		Radial basis—Radbas	
validation metric	Training	Testing	Training	Testing	Training	Testing
ME	− 0.0013	− 0.0003	− 0.0010	− 0.0035	0.0011	− 0.0021
MAE	0.0054	0.0064	0.0049	0.0066	0.0050	0.0071
MSE	0.0000	0.0001	0.0000	0.0001	0.0000	0.0001
RMSE	0.0068	0.0078	0.0064	0.0086	0.0063	0.0094
MRE	0.0279	0.0316	0.0239	0.0306	0.0240	0.0299
SD	0.0067	0.0080	0.0064	0.0080	0.0062	0.0094
SEM	0.0007	0.0017	0.0007	0.0017	0.0007	0.0020
R^2	0.9703	0.9662	0.9759	0.9730	0.9848	0.9783
adj. R^2	0.9711	0.9649	0.9746	0.9697	0.9843	0.9780

Fig. 16 Relative importance of different input variables for the COF for material (B) in garson, connection weights, most squares, and average RI
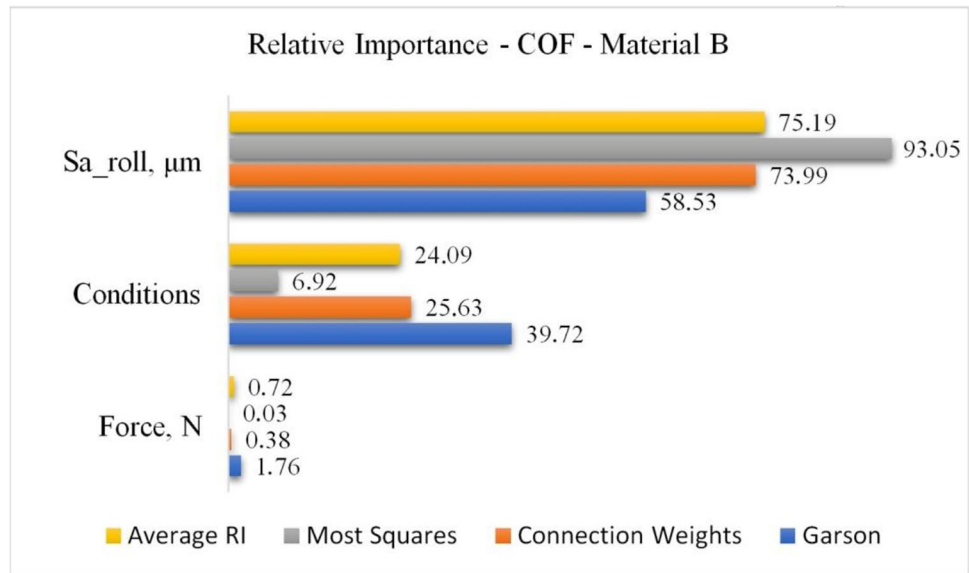
did not contain the training dataset. It is worth mentioning that conditions (dry or oil) were put in binary form and encoded using ordinal encoding. The so-called early stopping strategy enhanced generalisation in the MLP network developed to predict COF values in this study. All supervised network generation functions, including backpropagation networks, use the early stopping strategy as a default method. The training dataset is divided into three subsets: training, validation, and testing (Fig. 5).

Validating performance at each stage tries to fit the results and ensure that they conform with the pre-set goal at the desired level. Validation necessitates that performance meets or exceeds the goals set for the model. Figure 6 shows the matching results of training, validation, and test, which together and overall indicate the performance of the model once trained.

Several validation metrics are available, but selecting the right one is critical for evaluating a predictive model. This study examined and verified various training and transferring algorithms to evaluate the agreement between the actual and predicted values. Selecting the appropriate validation metric is critical and difficult for evaluating outcomes and eliminating errors. All models trained and tested in this study were compared based on their evaluation by using the relevant metrics to assess findings regarding test performance.

Fig. 17 Relative importance of different input variables for the COF for material (SB) in garson, connection weights, most squares, and average RI
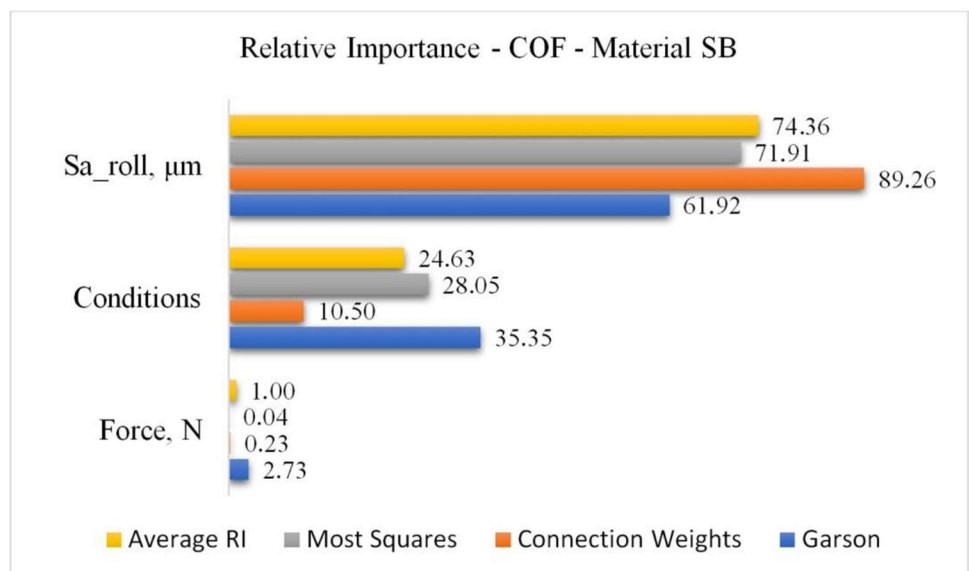
Fig. 18 Relative importance of different input variables for the COF for material (SSB) in garson, connection weights, most squares, and average RI
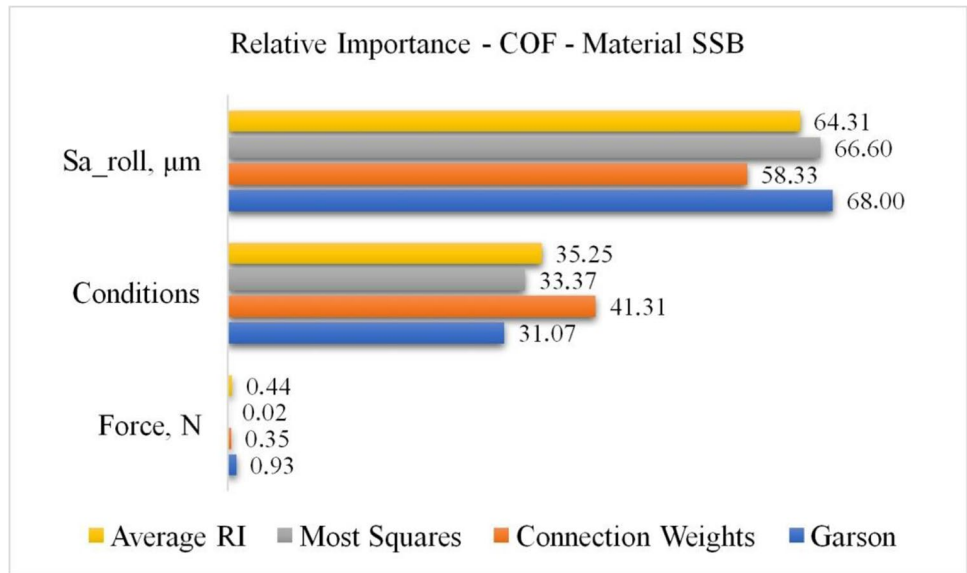
3 Results and discussion

3.1 ANN modelling

The best findings resulting from applying various models to forecast the COF have been summarised for Catboost and MLP, with the other detailed analyses presented in the Appendix. Tables 8, 9, and 10 show the values of several validation metrics used to check the performance of Catboost methods when materials B, SB, and SSB are utilised. The statistical parameters listed in these tables are as follows: ME, mean error; MAE, mean absolute error; MSE, mean square error; RMSE, root mean square error; MRE, mean relative error; SD, standard deviation; SEM, standard

error mean. R^2 and adj. R^2 are used to evaluate the models and structures in question, as an R^2 value near 1 indicates good performance. A situation where the MAE and RMSE values are close to 0 indicates that the model is performing well. Despite this, there are considerable differences in error distribution due to the significant variance between RMSE and MAE values. If MAE is more stable, RMSE is more vulnerable to error. Standard error mean SEM was used to validate the distribution of prediction values, where SEM is the standard deviation of the sampling distribution of the sample mean. In other words, sample mean variance is inversely proportional to sample size, and SEM is the SD of the original sample size over the square root of the sample size.

Fig. 19 Average relative importance of different input variables on COF for material (B), material (SB), and material (SSB)
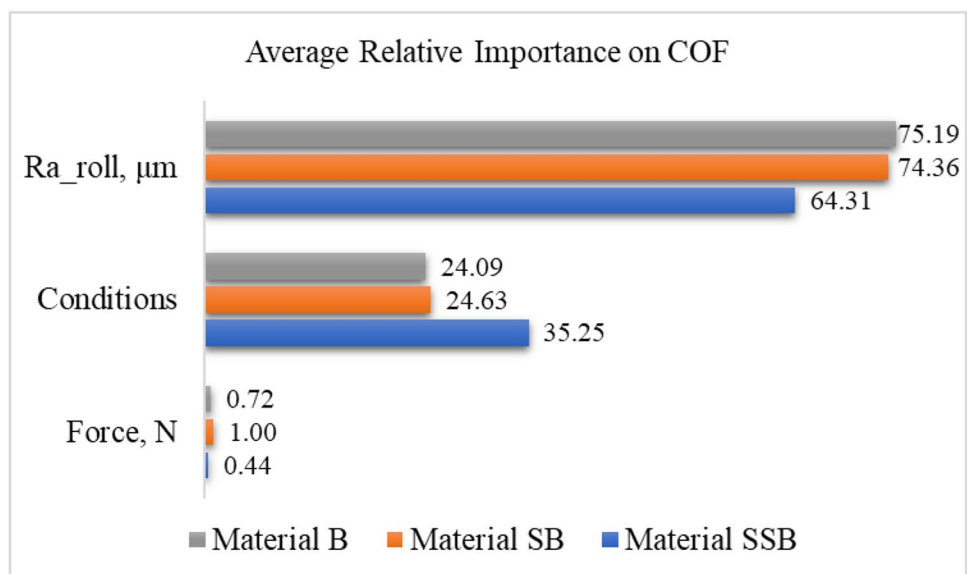
CatBoost is a competent tool that can predict various targets with default parameters. In this study, Catboost was able to predict the COF for material B with R^2 values of 0.9668 and 0.9281 for training and testing, respectively, as well as R^2 values of 0.9699 and 0.8426 for material SB and 0.9768 for training vis a vis 0.9224 for testing when predicting the COF for material SSB.

Figure 7 for material B, Fig. 8 for material SB, and Fig. 9 for materials SSB are the summary plot prediction of COF which highlights each feature's relevance to the other features' effects in the same row. The idea of Shapley additive explanations (SHAP) was to calculate the Shapley values for each feature of the sample as proposed by Lundberg and Lee [61], and its interpretation has been influenced by different methodologies [62–64]. Each point on the summary graphic indicates a feature's Shapley value. The feature's level is determined by axis Y, and Shapley values are displayed on axis X. The colour of the plots indicates the importance of the trait from low to high. The features are ordered by importance. The Shapley's values represent the relative distribution of predictions among the features. It is worth noting that identical values can contribute to different outputs depending on the values of other features in the same row.

On axis X, every data point in each dataset feature is represented as a single SHAP value, and each feature is represented on axis Y. The value of the feature is shown by the bar colour: red indicates high values, and blue shows low values. Grey points represent categorical inputs. The right-hand values have a "positive" effect on the output, whereas the left-hand values have a "negative" effect. Positive and negative are simply directional phrases that refer to how the model's output is influenced. However, they reflect the model's performance. For example, in the third row of Fig. 7, the most distant left point for force has a low value for the force feature in the third row. This low force has a -2 effect on COF as a model outcome. Without it, the predictive model would have anticipated a value of 2 or higher. Similarly, the lack of the rightmost bluepoint of the force with a value of 2 predicts a COF of -2 less. The most effective features are revealed by extending the data point further.

A SHAP decision plot, which uses cumulative SHAP values, was used to depict COF prediction models. Each line on the graph represents a single model prediction. All of the COF calculations are plotted in Figs. 10, 11, and 12.

As a result, this analysis demonstrates that each process condition is distinct and that various factors interact and have varying effects on individual results. Aside from cases of "dry" friction, conditions using different oils show variable COF. The same can be said for various forces and the Ra roll.

In other words, each value is represented individually; for example, Fig. 13 shows the total positive features values, Fig. 14 shows the total negative features values, and Fig. 15 shows combined positive and negative features values.

It is good to predict the results and expectations of the outcome of the experimental process before starting actual new experimental work using ANN techniques. Nevertheless, the ANN process requires the building of different structures and models, and most importantly, the prediction process cannot be carried out without previous actual data apart from the time of running. Predicting is a practical, cost-reducing, and effective method, but what if researchers want to predict new parameters without historical data? Instead of constructing, running, and evaluating a new ANN model each time, analytical equations for COF prediction were retrieved from the best model. As a result, a new method was developed; one of the novelties and emerging findings of this research is to develop a neural network structure based on training and transfer functions with different conditions to extract an equation for the prediction of COF from the best model that was implemented for the three different conditions. These equations can be used directly to predict the results by adding new parameters selected. Thus, Tables 12, 13, and 14 in the Appendix show the values of different validation metrics used to verify performance when predicting the COF for materials B, SB, and SSB, respectively, in various models.

It is critical to distinguish between test and training errors. The data used to train the model is utilised to calculate training errors, while the test error is derived using a whole dataset unknown to the model. The R^2 value of the training dataset reflects variance within the trained samples as a result of the model, and the R^2 value of the testing dataset indicates the model's predictive quality. Tables 12, 13, and 14 in the Appendix show that many models developed can predict the COF efficiently and accurately. However, When the R^2 of the testing was compared between the algorithms, it was discovered that the Levenberg–Marquardt (LM)—Trainlm performed the best as a training function in predicting the COF for all the materials (B, SB, and SSB). Positive saturating linear—Satlin was the best as a transfer function to predict the COF for material B with R^2 values equal to 0.970 for training and 0.966 for testing. The radial basis transfer function produced the best prediction of the COF for the other two materials (SB and SSB), which shows the highest R^2 value as a model performance. As a result, Table 11 shows the results of various validation metrics used to evaluate the best algorithms for predicting the COF for materials B, SB, and SSB.

Equations (3) and (10) are satlin and radbas transfer functions. Equation (4) is the COF prediction equation for metal B before weights and biases, and Eq. (5) is the transfer function variable. Equation (5) into Eq. (4) produces Eq. (6). Equation (7) substitutes weights and biases, and Eq. (8) describes the outcomes. Equation (9) for predicting the COF of material

B using the best-performing ANN network's constant weights and biases. Equations (11) and (12) predict COF for metals SB and SSB before adding weights and biases. Consequently, Eqs. (13) and (14) were created for materials SB and SSB, requiring constant weights and biases from the best-performing ANN network. The ANN network weights and biases retrieved served as a single input weight (IW) and the layered weight (LW). The IW represents the connection between the inputs and the hidden layer, while the LW represents the connection between the hidden and output layers, and b_1/b_2 are the biases for each layer. Tables 15, 16, and 17 in the Appendix contain b_1, b_2, IW, and LW from the best trained ANN model for the COF for materials B, SB, and SSB, respectively. These equations can predict the COF with accuracies of 0.966, 0.974, and 0.981 as R^2 values for materials B, SB, and SSB. Table 18 summarises the actual and predicted values of the COF (training and testing sets) for materials B, SB, and SSB.

$$f(x) = satlin(x) = \begin{pmatrix} 0, & if \ x <= 0; \\ x, & if \ 0 <= x <= 1; \\ 1, & if \ 1 <= x. \end{pmatrix} \tag{3}$$

Material B:

$$Coefficient \ of \ friction_i^{predict} = b_2 + LW \times satlin(b_1 + IW \times x) \tag{4}$$

$$\bar{x} = satlin(b_1 + IW \times x) \tag{5}$$

$$Coefficient \ of \ friction_i^{predict} = b_2 + LW \times \bar{x} \tag{6}$$

$$\bar{x} = satlin \left(\begin{array}{c} b_1 \\ \begin{bmatrix} -0.5153 \\ 1.8021 \\ 2.0233 \\ 0.6134 \\ 0.8628 \\ 2.0542 \\ 1.0798 \\ 0.0882 \\ 1.9710 \\ -0.0544 \end{bmatrix} + \begin{bmatrix} IW \\ 0.0990 & -2.1423 & -0.3941 & -0.2760 & -0.1587 & -0.4130 & -0.1317 & -0.1427 & -2.7457 & 0.0075 \\ 0.0005 & 0.0194 & 0.0006 & 0.0025 & 0.0049 & -0.0702 & 0.0004 & -0.0005 & -0.0006 & 0.0001 \\ 0.5210 & 0.4194 & -0.2235 & 0.0209 & -0.3164 & -0.0126 & -0.3104 & 0.1254 & 0.1577 & 0.0129 \end{bmatrix} \times \begin{bmatrix} x \\ R\_roll, \mu m \\ Force, N \\ Conditions \end{bmatrix} \right) \tag{7}$$

$$\bar{x} = \begin{pmatrix} 0, & if \ x <= 0; \\ x, & if \ 0 <= x <= 1; \\ 1, & if \ 1 <= x. \end{pmatrix} \tag{8}$$

$$Coefficient \ of \ friction_i^{predict} = \begin{array}{c} b_2 \\ [0.1762] \end{array} + \begin{bmatrix} LW \\ -0.0028 & 0.0033 & 0.0659 & -0.1163 & 0.0134 & 0.0087 & 0.1075 & 0.1031 & -0.0481 & -0.2114 \end{bmatrix} \times \bar{x} \tag{9}$$

Material SB and material SSB:

$$f(x) = radbas(x) = exp^{-x^2} \tag{10}$$

$$Coefficient \ of \ friction_i^{predict} = b_2 + LW \times radbas(b_1 + IW \times x) \tag{11}$$

$$Coefficient \ of \ friction_i^{predict} = b_2 + LW \times exp^{-(b_1 + IW \times x)^2} \tag{12}$$

Material SB:

$$Coefficient\ of\ friction_i^{predict} = \overset{b_2}{[0.0462]} + \overset{LW}{\begin{bmatrix} 0.0591 & -0.0276 & 0.0122 & 0.0036 \\ -0.0373 & -0.9140 & 0.1753 \\ 0.0007 & 0.0134 & 0.0530 \end{bmatrix}}$$

$$-\left(\overset{b_1}{\begin{bmatrix} -2.7486 \\ 1.0488 \\ 12.4986 \\ 0.0792 \\ 4.8382 \\ 6.2705 \\ -0.0603 \\ 6.2339 \\ 0.9833 \\ -4.1847 \end{bmatrix}} + \overset{IW}{\begin{bmatrix} 0.9706 & -1.0311 & -8.2366 & 2.4506 & 2.2511 & -6.0934 & 0.1083 & -0.5598 & 8.6841 & 0.8066 \\ -0.0027 & -0.3357 & 0.0179 & -0.0127 & 0.0153 & -0.0014 & -0.0015 & -0.0019 & -0.2910 & 0.0022 \\ 0.0303 & 0.0313 & 0.9374 & -1.0886 & -1.1468 & 0.3067 & -0.1319 & -1.7073 & 15.9755 & 2.4511 \end{bmatrix}} \times \overset{x}{\begin{bmatrix} R\_roll, \mu m \\ Force, N \\ Conditions \end{bmatrix}} \right)$$

$$\times exp$$

(13)

Material SSB:

$$Coefficient\ of\ friction_i^{predict} = \overset{b_2}{[0.4451]} + \overset{LW}{\begin{bmatrix} -0.3456 & 0.0053 & 0.0350 & -0.0276 & -0.0032 & -0.0025 & 0.0342 & -0.0460 & 0.0023 & 0.0496 \end{bmatrix}}$$

$$-\left(\overset{b_1}{\begin{bmatrix} -0.6990 \\ 0.8577 \\ -8.2426 \\ -7.6214 \\ -7.7505 \\ -0.2955 \\ -1.5801 \\ 5.1172 \\ -5.6255 \\ 3.8252 \end{bmatrix}} + \overset{IW}{\begin{bmatrix} -0.1380 & -0.5129 & 3.3903 & 1.2286 & 2.1771 & 3.1502 & 1.2511 & 1.3836 & -1.8754 & -0.2856 \\ 0.0011 & -0.0147 & 0.0065 & -0.0010 & 0.0013 & 0.0173 & 0.0043 & -0.0197 & 0.1052 & -0.0001 \\ 0.0686 & -0.4789 & 0.4396 & 1.5300 & 1.4172 & -0.6911 & -0.0821 & -0.0138 & 0.1589 & -2.9979 \end{bmatrix}} \times \overset{x}{\begin{bmatrix} R\_roll, \mu m \\ Force, N \\ Conditions \end{bmatrix}} \right)$$

$$\times exp$$

(14)

3.2 Contribution analysis of input variables

A feature's contribution and the calculation of the contributions of the features that have been implemented to reach the prediction amounts to presenting the input variables and how they affect the output, which is the COF. A feature's importance, variable importance, or relative importance refers to the analysis of the contribution of input variables to the corresponding outputs. On the other hand, this study shows changes in the averages of predictions when the feature value changes, indicating the relative relevance of each feature in the model driving a prediction. When variables with lower relative importance (RI) values substitute high RI input variables, the outcomes are significantly different [54, 65, 66]. Garson [67], most squares [68], and connection weights [69] are some of the methods for calculating the importance of a feature. The importance of a feature calculated on the basis of these methods is established based on the connection weights of neurons and is depicted in Eqs. (7), (13), and (14), respectively, for materials B, SB, and SSB.

Figure 16, 17, and 18 indicate significant parameters impacting the COF in terms of relative importance and weight analysis, which explains how each feature contributes to and influences the model. This technique estimates each feature's contribution to each row of the dataset. Based on weights and biases for determining the contributions of input variables impacting output (COF), all approaches reveal that changes in Ra_roll and condition (dry or using oil) significantly affect the COF for the three types of materials, with minimal variance. Furthermore, nominal force is always ranked at the bottom of the importance list because it has an almost negligible impact. The average relative importance of different input variables on COF of all materials is shown in Fig. 19.

4 Conclusions

In this article, the CatBoost machine learning algorithm developed by Yandex researchers and engineers is used for modelling and parameter identification of the coefficient of friction for three grades of deep-drawing quality steel sheets. A Shapley's decision plot, which uses cumulative Shapley additive explanations (SHAP) values, was used to depict the COF prediction models. One of the emerging findings of this research is the value of developing a neural network structure based on training and transfer functions with different conditions to extract the equation for the prediction of COF from the best model that was implemented for the three different conditions. The following conclusions can be drawn from the research.

1. CatBoost was able to predict the coefficient of friction with R^2 values between 0.9668 and 0.9774 for the training dataset, between 0.8818 and 0.9324 for the testing dataset, and between 0.9574 and 0.9693 as an average for the training and testing dataset, depending on the grade of steel sheet.

2. It was discovered that, for all the materials tested, the Levenberg–Marquardt training algorithm performed the best in predicting the coefficient of friction.

3. As a result, this analysis demonstrates that each process condition is distinct and that various factors interact and have varying effects on individual results. Aside from cases of dry friction, conditions with different oils show a variable COF. The same can be said for various normal forces and the surface roughness of the countersamples.

4. The radial basis transfer function produced the best prediction of the COF for two materials SB and SSB. The positive saturating linear—Satlin transfer function provided the best COF prediction for material B with R^2 values greater than 0.96.

5. All approaches reveal that changes in the surface roughness of the countersamples and conditions (dry or using oil) significantly affect the COF for three types of materials, with minimal variance. Moreover, nominal force always has the almost negligible impact.

Appendix

Table 12 Validation metrics of all multilayer perceptron (MLP) models for predicting COF (material B)

Training function: Levenberg–Marquardt (LM)—Trainlm

Transfer function		Elliotsig	Hardlim	Hardlims	Logsig	Netinv	Poslin	Purelin	Radbas	Radbasn	Satlin	Satlins	Softmax	Tansig	Tribas
Training	R^2	0.9608	0.8644	0.8471	0.9627	0.9512	0.9412	0.8596	0.9676	0.9720	0.9703	0.9702	0.9457	0.9695	0.9617
	MSE	0.0001	0.0002	0.0002	0.0001	0.0001	0.0001	0.0002	0.0001	0.0000	0.0000	0.0000	0.0001	0.0000	0.0001
Testing	R^2	0.9518	0.7822	0.7982	0.9625	0.9485	0.9354	0.7975	0.9528	0.9124	0.9662	0.9687	0.9442	0.9551	0.9591
	MSE	0.0001	0.0003	0.0004	0.0001	0.0001	0.0001	0.0004	0.0001	0.0001	0.0001	0.0001	0.0001	0.0001	0.0001

Training function: BFGS quasi-Newton (BFG)—Trainbfg

Transfer function		Elliotsig	Hardlim	Hardlims	Logsig	Netinv	Poslin	Purelin	Radbas	Radbasn	Satlin	Satlins	Softmax	Tansig	Tribas
Training	R^2	0.9446	0.8953	0.8473	0.9399	0.9431	0.8501	0.8451	0.9394	0.9396	0.9164	0.8495	0.9423	0.9396	0.8285
	MSE	0.0001	0.0002	0.0002	0.0001	0.0001	0.0002	0.0002	0.0001	0.0001	0.0001	0.0002	0.0001	0.0001	0.0003
Testing	R^2	0.9352	0.8761	0.8298	0.9355	0.9413	0.8253	0.8426	0.8839	0.9216	0.9023	0.8323	0.9380	0.9166	0.8088
	MSE	0.0001	0.0002	0.0003	0.0001	0.0001	0.0003	0.0003	0.0001	0.0001	0.0002	0.0004	0.0001	0.0002	0.0003

Training function: Resilient backpropagation (RP)—Trainrp

Transfer function		Elliotsig	Hardlim	Hardlims	Logsig	Netinv	Poslin	Purelin	Radbas	Radbasn	Satlin	Satlins	Softmax	Tansig	Tribas
Training	R^2	0.9340	0.8893	0.8068	0.9360	0.9396	0.8628	0.8446	0.9318	0.9340	0.0000	0.9305	0.9422	0.9420	0.8688
	MSE	0.0001	0.0002	0.0003	0.0001	0.0001	0.0002	0.0002	0.0001	0.0001	0.0016	0.0001	0.0001	0.0001	0.0002
Testing	R^2	0.9318	0.7657	0.8014	0.9187	0.9387	0.7619	0.8413	0.9102	0.9166	-0.0004	0.9212	0.9337	0.9294	0.8643
	MSE	0.0001	0.0002	0.0003	0.0001	0.0001	0.0004	0.0003	0.0001	0.0001	0.0015	0.0001	0.0001	0.0001	0.0002

Training function: Scaled conjugate gradient (SCG)—Trainscg

Transfer function		Elliotsig	Hardlim	Hardlims	Logsig	Netinv	Poslin	Purelin	Radbas	Radbasn	Satlin	Satlins	Softmax	Tansig	Tribas
Training	R^2	0.9340	0.8192	0.8327	0.9422	0.9331	0.8447	0.8467	0.9365	0.9382	0.8998	0.8208	0.9307	0.9344	0.8992
	MSE	0.0001	0.0003	0.0003	0.0001	0.0001	0.0002	0.0002	0.0001	0.0001	0.0002	0.0003	0.0001	0.0001	0.0002
Testing	R^2	0.9272	0.8154	0.8214	0.8901	0.7945	0.8440	0.8392	0.9210	0.8608	0.8824	0.7891	0.9233	0.9340	0.8458
	MSE	0.0001	0.0003	0.0003	0.0001	0.0002	0.0002	0.0003	0.0001	0.0001	0.0002	0.0003	0.0001	0.0001	0.0002

Training function: Conjugate gradient with Powell-Beale restarts (CGB)—Traincgb

Transfer function		Elliotsig	Hardlim	Hardlims	Logsig	Netinv	Poslin	Purelin	Radbas	Radbasn	Satlin	Satlins	Softmax	Tansig	Tribas
Training	R^2	0.9336	0.8557	0.8243	0.9312	0.8997	0.8416	0.8579	0.9208	0.9239	0.8277	0.8506	0.8705	0.9478	0.7042
	MSE	0.0001	0.0002	0.0003	0.0001	0.0002	0.0002	0.0002	0.0001	0.0001	0.0003	0.0002	0.0002	0.0001	0.0005
Testing	R^2	0.9311	0.8429	0.8220	0.9214	0.8649	0.8399	0.7820	0.7345	0.8219	0.7605	0.7715	0.8452	0.9463	0.5117
	MSE	0.0001	0.0002	0.0003	0.0001	0.0002	0.0003	0.0003	0.0003	0.0002	0.0003	0.0004	0.0003	0.0001	0.0008

Training function: Conjugate gradient with Fletcher-Reeves updates (CGF)—Traincgf

Transfer function		Elliotsig	Hardlim	Hardlims	Logsig	Netinv	Poslin	Purelin	Radbas	Radbasn	Satlin	Satlins	Softmax	Tansig	Tribas
Training	R^2	0.9229	0.8454	0.8610	0.9163	0.8514	0.4827	-8.7249	0.8932	0.8982	0.8377	0.8529	0.8444	0.9224	0.4316
	MSE	0.0001	0.0002	0.0002	0.0001	0.0002	0.0008	0.0161	0.0002	0.0002	0.0003	0.0002	0.0002	0.0001	0.0009
Testing	R^2	0.9085	0.8311	0.8470	0.8998	0.8056	0.3972	-8.8385	0.8264	0.7825	0.8248	0.7765	0.8298	0.8551	0.2844
	MSE	0.0002	0.0003	0.0003	0.0002	0.0002	0.0010	0.0134	0.0002	0.0003	0.0003	0.0004	0.0002	0.0002	0.0014

Table 12 (continued)

Training funtion		Levenberg–Marquardt (LM)—Trainlm													
Transfer function		Elliotsig	Hardlim	Hardlims	Logsig	Netinv	Poslin	Purelin	Radbas	Radbasn	Satlin	Satlins	Softmax	Tansig	Tribas
Training funtion		Conjugate gradient with Polak-Ribiére updates (CGP)—Traincgp													
Training	R^2	0.9321	0.8854	0.8797	0.9371	0.8526	0.7640	0.5258	0.9376	0.8769	0.8532	0.8402	0.8437	0.9125	0.6341
	MSE	0.0001	0.0002	0.0002	0.0001	0.0002	0.0004	0.0008	0.0001	0.0002	0.0002	0.0003	0.0002	0.0001	0.0006
Testing	R^2	0.9038	0.8186	0.8677	0.9035	0.8200	0.7049	0.3596	0.8130	0.8736	0.7578	0.7879	0.8310	0.9019	0.5937
	MSE	0.0001	0.0003	0.0003	0.0001	0.0002	0.0002	0.0006	0.0002	0.0002	0.0003	0.0004	0.0003	0.0002	0.0007
Training funtion		One step secant (OSS)—Trainoss													
Training	R^2	0.9129	0.8210	0.8666	0.9325	0.9085	0.8992	0.8666	0.8699	0.7326	0.8509	0.8221	0.9288	0.8787	0.8501
	MSE	0.0001	0.0003	0.0002	0.0001	0.0001	0.0002	0.0002	0.0002	0.0004	0.0003	0.0003	0.0001	0.0002	0.0003
Testing	R^2	0.8742	0.8137	0.8367	0.8757	0.8545	0.8693	0.7318	0.8336	0.6920	0.8218	0.8043	0.8967	0.7544	0.6995
	MSE	0.0002	0.0003	0.0002	0.0002	0.0003	0.0002	0.0004	0.0003	0.0006	0.0002	0.0003	0.0002	0.0003	0.0003
Training funtion		Gradient descent with momentum and adaptive learning rate (GDX)—Traingdx													
Training	R^2	0.9258	0.8658	0.8380	0.9000	0.8219	0.8277	-	0.6536	0.6883	0.8207	0.8460	0.7942	0.7827	0.6428
	MSE	0.0001	0.0002	0.0003	0.0002	0.0003	0.0003	-	0.0006	0.0005	0.0003	0.0002	0.0004	0.0004	0.0006
Testing	R^2	0.8855	0.8584	0.7891	0.7630	0.7765	0.7434	-	0.6218	0.6679	0.7662	0.7387	0.6789	0.7812	0.6346
	MSE	0.0002	0.0002	0.0003	0.0003	0.0004	0.0003	-	0.0005	0.0004	0.0004	0.0004	0.0003	0.0003	0.0005
Training funtion		Bayesian regularisation backpropagation (BRB)—Ttrainbr													
Training	R^2	0.9660	0.8767	0.8936	0.9456	0.9604	0.9187	0.8524	0.9431	0.9481	0.9553	0.9392	0.9463	0.9470	0.9359
	MSE	0.0001	0.0002	0.0002	0.0001	0.0001	0.0001	0.0002	0.0001	0.0001	0.0001	0.0001	0.0001	0.0001	0.0001
Testing	R^2	0.9444	0.8228	0.8051	0.9377	0.9595	0.9076	0.8129	0.9396	0.9448	0.9184	0.9095	0.9306	0.9395	0.8999
	MSE	0.0001	0.0002	0.0003	0.0001	0.0001	0.0001	0.0003	0.0001	0.0001	0.0002	0.0001	0.0001	0.0001	0.0001

Table 13 Validation metrics of all multilayer perceptron (MLP) models for predicting COF (material SB)

Transfer function		Elliotsig	Hardlim	Hardlims	Logsig	Netinv	Poslin	Purelin	Radbas	Radbasn	Satlin	Satlins	Softmax	Tansig	Tribas
Training funtion	**Levenberg–Marquardt (LM)—Trainlm**														
Training	R^2	0.9628	0.8860	0.9012	0.9806	0.9555	0.9622	0.9261	0.9759	0.9800	0.9722	0.9699	0.9577	0.9831	0.9736
	MSE	0.0001	0.0002	0.0002	0.0000	0.0001	0.0001	0.0001	0.0000	0.0000	0.0001	0.0001	0.0001	0.0000	0.0000
Testing	R^2	0.9626	0.8756	0.8457	0.9622	0.9159	0.9610	0.8786	0.9730	0.9678	0.9705	0.9626	0.9052	0.9624	0.9688
	MSE	0.0001	0.0003	0.0002	0.0001	0.0001	0.0001	0.0003	0.0001	0.0001	0.0001	0.0001	0.0001	0.0001	0.0001
Training funtion	**BFGS quasi-Newton (BFG)—Trainbfg**														
Training	R^2	0.9494	0.8900	0.8794	0.9548	0.9461	0.9182	0.9220	0.9487	0.9425	0.9202	0.9165	0.9315	0.9491	0.9239
	MSE	0.0001	0.0002	0.0002	0.0001	0.0001	0.0002	0.0002	0.0001	0.0001	0.0002	0.0001	0.0001	0.0001	0.0001
Testing	R^2	0.9487	0.8804	0.8697	0.9362	0.9419	0.9125	0.8475	0.9081	0.9201	0.9107	0.9073	0.9301	0.9423	0.9057
	MSE	0.0001	0.0002	0.0002	0.0001	0.0001	0.0001	0.0002	0.0002	0.0001	0.0002	0.0002	0.0002	0.0001	0.0002
Training funtion	**Resilient backpropagation (RP)—Trainrp**														
Training	R^2	0.9521	0.8929	0.9033	0.9498	0.9545	0.9193	0.9195	0.9509	0.9551	-0.0004	0.9510	0.9473	0.9502	0.9417
	MSE	0.0001	0.0002	0.0002	0.0001	0.0001	0.0001	0.0002	0.0001	0.0001	0.0019	0.0001	0.0001	0.0001	0.0001
Testing	R^2	0.9036	0.8864	0.8490	0.9082	0.9516	0.9067	0.9008	0.9086	0.9170	-0.0017	0.9120	0.9387	0.9322	0.9276
	MSE	0.0002	0.0003	0.0003	0.0001	0.0001	0.0002	0.0002	0.0001	0.0001	0.0020	0.0001	0.0001	0.0001	0.0002
Training funtion	**Scaled conjugate gradient (SCG)—Trainscg**														
Training	R^2	0.9483	0.9021	0.9059	0.9503	0.9334	0.9172	0.9190	0.9462	0.9417	0.9314	0.9445	0.9341	0.9500	0.9058
	MSE	0.0001	0.0002	0.0002	0.0001	0.0001	0.0002	0.0001	0.0001	0.0001	0.0001	0.0001	0.0001	0.0001	0.0002
Testing	R^2	0.9200	0.8639	0.8682	0.9503	0.9064	0.9126	0.9038	0.8808	0.9294	0.8973	0.8926	0.9057	0.9296	0.8648
	MSE	0.0002	0.0002	0.0002	0.0001	0.0002	0.0001	0.0002	0.0002	0.0002	0.0002	0.0002	0.0002	0.0001	0.0002
Training funtion	**Conjugate gradient with Powell-Beale restarts (CGB)—Traincgb**														
Training	R^2	0.9464	0.9034	0.9299	0.9499	0.8825	0.9226	0.9240	0.9493	0.9084	0.9044	0.9406	0.9182	0.9392	0.7459
	MSE	0.0001	0.0002	0.0001	0.0001	0.0002	0.0002	0.0002	0.0001	0.0002	0.0002	0.0001	0.0002	0.0001	0.0005
Testing	R^2	0.9414	0.8490	0.8884	0.8922	0.8642	0.8765	0.8511	0.9031	0.8871	0.9031	0.8938	0.8793	0.9357	0.7126
	MSE	0.0001	0.0004	0.0002	0.0002	0.0002	0.0002	0.0002	0.0001	0.0003	0.0002	0.0002	0.0002	0.0002	0.0006
Training funtion	**Conjugate gradient with Fletcher-Reeves updates (CGF)—Traincgf**														
Training	R^2	0.9466	0.9068	0.9030	0.9450	0.8595	0.0633	0.7346	0.9450	0.9495	0.8519	0.9248	0.9226	0.9195	0.6163
	MSE	0.0001	0.0002	0.0002	0.0001	0.0003	0.0018	0.0005	0.0001	0.0001	0.0003	0.0002	0.0002	0.0002	0.0007
Testing	R^2	0.8970	0.8776	0.8636	0.9319	0.8548	0.0441	0.6377	0.8042	0.7851	0.7206	0.8795	0.9117	0.9171	0.5561
	MSE	0.0002	0.0003	0.0002	0.0002	0.0002	0.0017	0.0007	0.0003	0.0004	0.0005	0.0002	0.0001	0.0001	0.0009
Training funtion	**Conjugate gradient with Polak-Ribiére updates (CGP)—Traincgp**														
Training	R^2	0.9424	0.9064	0.8791	0.9453	0.8737	0.9267	0.8885	0.9428	0.9065	0.9045	0.8793	0.8830	0.9441	0.6755
	MSE	0.0001	0.0002	0.0002	0.0001	0.0002	0.0001	0.0002	0.0001	0.0002	0.0002	0.0002	0.0002	0.0001	0.0006
Testing	R^2	0.9229	0.8776	0.8419	0.8826	0.8718	0.8043	0.8847	0.8506	0.8448	0.8441	0.8188	0.8791	0.9300	0.6295
	MSE	0.0001	0.0003	0.0002	0.0002	0.0003	0.0003	0.0002	0.0003	0.0002	0.0002	0.0004	0.0002	0.0002	0.0007

Table 13 (continued)

Training funtion	Levenberg–Marquardt (LM)—Trainlm													
Transfer function	Elliotsig	Hardlim	Hardlims	Logsig	Netinv	Poslin	Purelin	Radbas	Radbasn	Satlin	Satlins	Softmax	Tansig	Tribas
Training funtion	**One step secant (OSS)—Trainoss**													
Training R^2	0.9513	0.9004	0.8864	0.9340	0.9356	0.9188	0.9269	0.9188	0.9341	0.9378	0.9201	0.9281	0.9305	0.3969
MSE	0.0001	0.0002	0.0002	0.0001	0.0001	0.0001	0.0001	0.0002	0.0001	0.0001	0.0001	0.0001	0.0001	0.0012
Testing R^2	0.9085	0.8830	0.8445	0.9036	0.8853	0.9017	0.8693	0.9121	0.8832	0.9192	0.8762	0.9278	0.8371	0.3261
MSE	0.0001	0.0002	0.0004	0.0002	0.0002	0.0002	0.0003	0.0002	0.0002	0.0002	0.0002	0.0001	0.0002	0.0011
Training funtion	**Gradient descent with momentum and adaptive learning rate (GDX)—Traingdx**													
Training R^2	0.8905	0.8803	0.8812	0.9399	0.8754	0.8901	-	0.6560	0.7636	0.8045	0.8674	0.9040	0.8911	0.7408
MSE	0.0002	0.0002	0.0002	0.0001	0.0003	0.0002	-	0.0007	0.0005	0.0004	0.0002	0.0002	0.0002	0.0005
Testing R^2	0.8693	0.8732	0.8394	0.9009	0.8443	0.8551	-	0.5855	0.6350	0.7840	0.7816	0.8866	0.8275	0.6796
MSE	0.0003	0.0003	0.0003	0.0002	0.0002	0.0003	-	0.0006	0.0007	0.0003	0.0005	0.0002	0.0002	0.0006
Training funtion	**Bayesian regularisation backpropagation (BRB)—Ttrainbr**													
Training R^2	0.9546	0.9070	0.9262	0.9530	0.9562	0.9464	0.9228	0.9552	0.9548	0.9518	0.9202	0.9464	0.9473	0.9312
MSE	0.0001	0.0002	0.0001	0.0001	0.0001	0.0001	0.0001	0.0001	0.0001	0.0001	0.0002	0.0001	0.0001	0.0001
Testing R^2	0.9454	0.9049	0.9259	0.9525	0.9515	0.9441	0.8938	0.9524	0.9517	0.9295	0.9151	0.9309	0.9390	0.9209
MSE	0.0001	0.0002	0.0001	0.0001	0.0001	0.0001	0.0002	0.0001	0.0001	0.0001	0.0001	0.0001	0.0001	0.0002

Table 14 Validation metrics of all multilayer perceptron models for predicting COF (material SSB)

Training funtion		Elliotsig	Hardlim	Hardlims	Logsig	Netinv	Poslin	Purelin	Radbas	Radbasn	Satlin	Satlins	Softmax	Tansig	Tribas
Transfer function															
Levenberg–Marquardt (LM)—Trainlm															
Training	R^2	0.9702	0.8789	0.9014	0.9815	0.9664	0.9731	0.8939	0.9848	0.9833	0.9780	0.9818	0.9728	0.9781	0.9794
	MSE	0.0001	0.0003	0.0003	0.0000	0.0001	0.0001	0.0003	0.0000	0.0001	0.0001	0.0001	0.0001	0.0001	0.0001
Testing	R^2	0.9661	0.8358	0.8715	0.9703	0.9551	0.9628	0.8848	0.9783	0.9665	0.9717	0.9641	0.9625	0.9714	0.9622
	MSE	0.0001	0.0005	0.0004	0.0001	0.0001	0.0001	0.0003	0.0001	0.0001	0.0001	0.0001	0.0001	0.0001	0.0001
BFGS quasi-Newton (BFG)—Trainbfg															
Training	R^2	0.9666	0.8816	0.8712	0.9644	0.9680	0.8928	0.9039	0.9557	0.9646	0.9567	0.9249	0.9635	0.9516	0.9019
	MSE	0.0001	0.0004	0.0004	0.0001	0.0001	0.0003	0.0003	0.0001	0.0001	0.0001	0.0002	0.0001	0.0001	0.0003
Testing	R^2	0.9624	0.8304	0.8569	0.9628	0.9579	0.8826	0.8275	0.9291	0.9628	0.9229	0.8824	0.9389	0.9492	0.8510
	MSE	0.0001	0.0004	0.0005	0.0001	0.0001	0.0003	0.0004	0.0002	0.0001	0.0002	0.0004	0.0002	0.0002	0.0003
Resilient backpropagation (RP)—Trainrp															
Training	R^2	0.9633	0.9136	0.8850	0.9663	0.9639	0.9367	0.8942	0.9661	0.9684	0.0000	0.9641	0.9655	0.9687	0.9584
	MSE	0.0001	0.0003	0.0003	0.0001	0.0001	0.0002	0.0003	0.0001	0.0001	0.0026	0.0001	0.0001	0.0001	0.0001
Testing	R^2	0.9421	0.8538	0.8457	0.9358	0.9482	0.8854	0.8866	0.9556	0.9380	-0.0001	0.9516	0.9492	0.9137	0.9262
	MSE	0.0002	0.0003	0.0006	0.0002	0.0002	0.0003	0.0003	0.0001	0.0001	0.0039	0.0001	0.0001	0.0002	0.0002
Scaled conjugate gradient (SCG)—Trainscg															
Training	R^2	0.9592	0.8721	0.8962	0.9650	0.9460	0.9125	0.8917	0.9646	0.9452	0.9337	0.9406	0.9469	0.9598	0.8797
	MSE	0.0001	0.0004	0.0003	0.0001	0.0002	0.0002	0.0003	0.0001	0.0002	0.0002	0.0002	0.0002	0.0001	0.0004
Testing	R^2	0.9364	0.8567	0.8463	0.9514	0.9408	0.8730	0.8915	0.8900	0.9267	0.9316	0.9361	0.9209	0.9551	0.7473
	MSE	0.0002	0.0004	0.0004	0.0001	0.0002	0.0004	0.0003	0.0002	0.0001	0.0002	0.0002	0.0002	0.0001	0.0003
Conjugate gradient with Powell-Beale restarts (CGB)—Traincgb															
Training	R^2	0.9648	0.9139	0.8805	0.9657	0.9303	0.9104	0.8880	0.9458	0.9637	0.8940	0.8964	0.9134	0.9654	0.5206
	MSE	0.0001	0.0002	0.0004	0.0001	0.0002	0.0003	0.0003	0.0002	0.0001	0.0003	0.0003	0.0003	0.0001	0.0014
Testing	R^2	0.9198	0.8748	0.8425	0.9322	0.9082	0.7890	0.8759	0.9323	0.9378	0.8791	0.8760	0.8334	0.9563	0.5076
	MSE	0.0002	0.0005	0.0004	0.0001	0.0002	0.0005	0.0003	0.0002	0.0002	0.0003	0.0003	0.0004	0.0001	0.0014
Conjugate gradient with Fletcher-Reeves updates (CGF)—Traincgf															
Training	R^2	0.9454	0.8751	0.9043	0.9617	0.9211	0.4303	-12.7086	0.9004	0.9433	0.8339	0.8969	0.9126	0.9487	0.4764
	MSE	0.0002	0.0004	0.0003	0.0001	0.0002	0.0017	0.0399	0.0003	0.0002	0.0005	0.0003	0.0002	0.0002	0.0015
Testing	R^2	0.9369	0.8089	0.8274	0.9476	0.8831	0.3311	-12.7738	0.8295	0.8673	0.8241	0.8320	0.8619	0.9324	0.2973
	MSE	0.0002	0.0004	0.0004	0.0001	0.0003	0.0015	0.0361	0.0004	0.0003	0.0004	0.0006	0.0004	0.0002	0.0022
PConjugate gradient with Polak-Ribiére updates (CGP)—Traincgp															
Training	R^2	0.9457	0.8706	0.8988	0.9670	0.8979	0.8033	0.6240	0.9310	0.9402	0.8983	0.8803	0.9322	0.9484	0.6373
	MSE	0.0002	0.0004	0.0003	0.0001	0.0003	0.0005	0.0011	0.0002	0.0002	0.0003	0.0003	0.0002	0.0001	0.0010
Testing	R^2	0.9220	0.8406	0.8870	0.9303	0.8840	0.7544	0.4519	0.9005	0.8696	0.8583	0.8578	0.8793	0.9279	0.5754
	MSE	0.0002	0.0005	0.0003	0.0002	0.0002	0.0011	0.0012	0.0002	0.0003	0.0004	0.0004	0.0004	0.0002	0.0014
One step secant (OSS)—Trainoss															

Table 14 (continued)

Training funtion		Levenberg–Marquardt (LM)—Trainlm												
Transfer function		Elliotsig	Hardlim	Hardlims	Logsig	Netinv	Poslin	Purelin	Radbas	Radbasn	Satlin	Satlins	Softmax	Tansig	Tribas
Training	R^2	0.9456	0.8832	0.8927	0.9558	0.9453	0.9122	0.9061	0.9032	0.8870	0.8996	0.8948	0.9477	0.9349	0.4965
	MSE	0.0002	0.0003	0.0003	0.0001	0.0002	0.0002	0.0002	0.0003	0.0003	0.0003	0.0003	0.0002	0.0002	0.0014
Testing	R^2	0.9392	0.8483	0.8496	0.9051	0.9221	0.8277	0.8519	0.9002	0.8051	0.8745	0.8942	0.9333	0.9248	0.4721
	MSE	0.0002	0.0003	0.0004	0.0003	0.0002	0.0006	0.0006	0.0002	0.0005	0.0004	0.0003	0.0002	0.0002	0.0018
Training funtion		Gradient descent with momentum and adaptive learning rate (GDX)—Traingdx													
Training	R^2	0.9310	0.8925	0.8797	0.9405	0.8698	0.8906	-2.3014	0.6854	0.6159	0.7901	0.8707	0.9023	0.8654	0.6598
	MSE	0.0002	0.0003	0.0003	0.0002	0.0004	0.0003	0.0092	0.0008	0.0011	0.0007	0.0004	0.0003	0.0004	0.0010
Testing	R^2	0.8363	0.8513	0.8455	0.8853	0.7941	0.7981	-2.4559	0.6341	0.6086	0.7552	0.7791	0.7940	0.8223	0.6388
	MSE	0.0004	0.0004	0.0005	0.0004	0.0005	0.0004	0.0111	0.0014	0.0010	0.0004	0.0006	0.0004	0.0004	0.0011
Training funtion		Bayesian regularisation backpropagation (BRB)—Ttrainbr													
Training	R^2	0.9712	0.8924	0.9003	0.9679	0.9664	0.9403	0.9060	0.9684	0.9679	0.9660	0.9738	0.9708	0.9673	0.9635
	MSE	0.0001	0.0003	0.0003	0.0001	0.0001	0.0002	0.0002	0.0001	0.0001	0.0001	0.0001	0.0001	0.0001	0.0001
Testing	R^2	0.9638	0.8905	0.8837	0.9645	0.9540	0.9188	0.8577	0.9642	0.9671	0.9583	0.9651	0.9641	0.9640	0.9409
	MSE	0.0001	0.0003	0.0003	0.0001	0.0001	0.0002	0.0006	0.0001	0.0001	0.0001	0.0001	0.0001	0.0001	0.0002

Table 15 Weights and biases of the best MLP model for predicting COF (Trainlm with Satlin—material B)

b_1	b_2	IW		LW	
−0.5153	0.1762	0.0990	0.0005	0.5210	−0.0028
1.8021		−2.1423	0.0194	0.4194	0.0033
2.0233		−0.3941	0.0006	−0.2235	0.0659
0.6134		−0.2760	0.0025	0.0209	−0.1163
0.8628		−0.1587	0.0049	−0.3164	0.0134
2.0542		−0.4130	−0.0702	−0.0126	0.0087
1.0798		−0.1317	0.0004	−0.3104	0.1075
0.0882		−0.1427	−0.0005	0.1254	0.1031
1.9710		−2.7457	−0.0006	0.1577	−0.0481
−0.0544		0.0075	0.0001	0.0129	−0.2114

Table 16 Weights and biases of the best MLP model for predicting COF (Trainlm with Rsdbas—material SB)

b_1	b_2	IW		LW	
−2.7486	0.0462	0.9706	−0.0027	0.0303	0.0591
1.0488		−1.0311	−0.3357	0.0313	−0.0276
12.4986		−8.2366	0.0179	0.9374	0.0122
0.0792		2.4506	−0.0127	−1.0886	0.0036
4.8382		2.2511	0.0153	−1.1468	−0.0373
6.2705		−6.0934	−0.0014	0.3067	−0.9140
−0.0603		0.1083	−0.0015	−0.1319	0.1753
6.2339		−0.5598	−0.0019	−1.7073	0.0007
0.9833		8.6841	−0.2910	15.9755	0.0134
−4.1847		0.8066	0.0022	2.4511	0.0530

Table 17 Weights and biases of the best MLP model for predicting COF (Trainlm with Rsdbas—material SSB)

b_1	b_2	IW		LW	
−0.6990	0.4451	−0.1380	0.0011	0.0686	−0.3456
0.8577		−0.5129	−0.0147	−0.4789	0.0053
−8.2426		3.3903	0.0065	0.4396	0.0350
−7.6214		1.2286	−0.0010	1.5300	−0.0276
−7.7505		2.1771	0.0013	1.4172	−0.0032
−0.2955		3.1502	0.0173	−0.6911	−0.0025
−1.5801		1.2511	0.0043	−0.0821	0.0342
5.1172		1.3836	−0.0197	−0.0138	−0.0460
−5.6255		−1.8754	0.1052	0.1589	0.0023
3.8252		−0.2856	−0.0001	−2.9979	0.0496

Table 18 All actual and predicted values of COF (training and testing sets) for materials B, SB, and SSB

Training							Testing						
S	Material B		Material SB		Material SSB		S	Material B		Material SB		Material SSB	
	Actual	Predicted	Actual	Predicted	Actual	Predicted		Actual	Predicted	Actual	Predicted	Actual	Predicted
1	0.263	0.256	0.158	0.157	0.302	0.297	91	0.248	0.242	0.184	0.181	0.339	0.349
2	0.228	0.226	0.200	0.208	0.225	0.227	92	0.131	0.126	0.173	0.177	0.146	0.144
3	0.147	0.143	0.221	0.219	0.164	0.166	93	0.279	0.261	0.164	0.169	0.309	0.293
4	0.216	0.204	0.270	0.267	0.247	0.243	94	0.280	0.277	0.175	0.174	0.245	0.254
5	0.200	0.196	0.231	0.223	0.378	0.380	95	0.200	0.193	0.270	0.260	0.232	0.230
6	0.212	0.210	0.226	0.218	0.213	0.205	96	0.255	0.244	0.143	0.140	0.210	0.207
7	0.205	0.202	0.191	0.194	0.195	0.199	97	0.192	0.202	0.157	0.154	0.154	0.155
8	0.158	0.152	0.164	0.169	0.186	0.194	98	0.188	0.175	0.176	0.177	0.244	0.233
9	0.196	0.187	0.206	0.200	0.270	0.267	99	0.169	0.169	0.138	0.136	0.152	0.147
10	0.207	0.220	0.214	0.216	0.148	0.147	100	0.235	0.234	0.157	0.164	0.358	0.364
11	0.167	0.172	0.274	0.265	0.150	0.156	101	0.257	0.264	0.280	0.277	0.213	0.220
12	0.228	0.228	0.152	0.152	0.168	0.173	102	0.180	0.185	0.199	0.199	0.182	0.183
13	0.240	0.250	0.241	0.227	0.171	0.172	103	0.227	0.234	0.178	0.183	0.219	0.215
14	0.164	0.157	0.228	0.233	0.178	0.172	104	0.156	0.159	0.300	0.281	0.168	0.169
15	0.168	0.169	0.148	0.143	0.157	0.158	105	0.191	0.193	0.139	0.129	0.305	0.280
16	0.164	0.164	0.246	0.228	0.199	0.206	106	0.230	0.228	0.242	0.228	0.226	0.219
17	0.173	0.160	0.202	0.189	0.238	0.240	107	0.175	0.186	0.326	0.311	0.288	0.276
18	0.171	0.176	0.222	0.212	0.218	0.215	108	0.187	0.179	0.200	0.204	0.166	0.185
19	0.223	0.226	0.195	0.198	0.259	0.260	109	0.202	0.206	0.226	0.235	0.290	0.286
20	0.257	0.264	0.239	0.237	0.273	0.262	110	0.136	0.140	0.214	0.211	0.131	0.133
21	0.264	0.257	0.140	0.133	0.214	0.222	111	0.207	0.220	0.210	0.206	0.189	0.187
22	0.272	0.268	0.227	0.228	0.196	0.198	112	0.147	0.149	0.248	0.229	0.252	0.244
23	0.222	0.221	0.244	0.240	0.201	0.198							
24	0.274	0.278	0.150	0.149	0.168	0.173							
25	0.164	0.168	0.210	0.213	0.240	0.245							
26	0.165	0.159	0.198	0.186	0.310	0.301							
27	0.207	0.196	0.266	0.268	0.193	0.205							
28	0.190	0.179	0.160	0.162	0.176	0.180							
29	0.239	0.235	0.222	0.222	0.324	0.326							
30	0.187	0.186	0.166	0.163	0.234	0.233							
31	0.154	0.143	0.182	0.189	0.169	0.176							
32	0.205	0.201	0.236	0.252	0.209	0.205							
33	0.282	0.265	0.234	0.225	0.207	0.205							
34	0.164	0.162	0.181	0.180	0.190	0.189							
35	0.178	0.173	0.191	0.177	0.180	0.173							
36	0.275	0.273	0.164	0.168	0.307	0.315							
37	0.258	0.258	0.187	0.176	0.260	0.238							
38	0.219	0.217	0.212	0.213	0.268	0.268							
39	0.142	0.139	0.295	0.287	0.214	0.213							
40	0.283	0.282	0.178	0.185	0.258	0.266							
41	0.128	0.126	0.170	0.170	0.231	0.240							
42	0.166	0.167	0.187	0.189	0.170	0.171							
43	0.173	0.166	0.219	0.218	0.229	0.222							
44	0.241	0.251	0.173	0.169	0.266	0.268							
45	0.166	0.160	0.143	0.147	0.300	0.299							
46	0.210	0.205	0.267	0.266	0.232	0.229							
47	0.183	0.185	0.178	0.187	0.280	0.287							

Table 18 (continued)

	Training							Testing						
S	Material B		Material SB		Material SSB			*S*	Material B		Material SB		Material SSB	
	Actual	Predicted	Actual	Predicted	Actual	Predicted			Actual	Predicted	Actual	Predicted	Actual	Predicted
48	0.164	0.154	0.282	0.277	0.169	0.183								
49	0.197	0.203	0.210	0.210	0.220	0.219								
50	0.282	0.272	0.200	0.200	0.162	0.163								
51	0.145	0.142	0.295	0.296	0.220	0.220								
52	0.172	0.176	0.252	0.260	0.190	0.197								
53	0.216	0.213	0.162	0.161	0.136	0.140								
54	0.153	0.151	0.188	0.193	0.163	0.165								
55	0.145	0.145	0.214	0.216	0.228	0.229								
56	0.227	0.225	0.206	0.207	0.249	0.250								
57	0.205	0.209	0.223	0.223	0.234	0.225								
58	0.148	0.150	0.243	0.242	0.255	0.252								
59	0.158	0.153	0.184	0.176	0.180	0.183								
60	0.185	0.166	0.136	0.147	0.149	0.142								
61	0.188	0.194	0.158	0.160	0.243	0.252								
62	0.161	0.163	0.190	0.185	0.207	0.212								
63	0.199	0.200	0.174	0.173	0.141	0.151								
64	0.195	0.207	0.260	0.248	0.214	0.206								
65	0.145	0.137	0.220	0.223	0.198	0.193								
66	0.193	0.210	0.223	0.218	0.225	0.218								
67	0.244	0.240	0.202	0.203	0.237	0.234								
68	0.185	0.175	0.204	0.212	0.261	0.267								
69	0.186	0.192	0.326	0.317	0.191	0.183								
70	0.184	0.195	0.181	0.180	0.232	0.235								
71	0.199	0.192	0.186	0.193	0.244	0.251								
72	0.132	0.131	0.255	0.245	0.137	0.141								
73	0.185	0.194	0.199	0.194	0.345	0.340								
74	0.273	0.269	0.254	0.253	0.312	0.312								
75	0.173	0.173	0.267	0.260	0.336	0.330								
76	0.159	0.165	0.146	0.150	0.221	0.230								
77	0.233	0.233	0.228	0.226	0.234	0.246								
78	0.174	0.185	0.265	0.271	0.150	0.154								
79	0.212	0.213	0.215	0.219	0.183	0.188								
80	0.220	0.215	0.145	0.154	0.276	0.277								
81	0.199	0.199	0.218	0.218	0.210	0.213								
82	0.176	0.182	0.307	0.304	0.185	0.192								
83	0.182	0.179	0.168	0.165	0.166	0.159								
84	0.233	0.243	0.220	0.220	0.284	0.288								
85	0.229	0.221	0.215	0.209	0.179	0.188								
86	0.274	0.270	0.181	0.194	0.244	0.242								
87	0.166	0.159	0.236	0.244	0.225	0.226								
88	0.172	0.168	0.167	0.166	0.280	0.278								
89	0.206	0.212	0.278	0.274	0.180	0.194								
90	0.168	0.171	0.220	0.223	0.199	0.208								

Data availability The data presented in this study are available on request from the corresponding author.

Declarations

Ethics approval Not applicable.

Consent to participate Not applicable.

Conflict of interest The authors declare no competing interests.

References

1. Dou S, Xia J (2019) Analysis of sheet metal forming (stamping process): a study of the variable friction coefficient on 5052 aluminum alloy. Metals (Basel) 9(8):853. https://doi.org/10.3390/met9080853

2. Dou S, Wang X, Xia J, Wilson L (2020) Analysis of sheet metal forming (warm stamping process): a study of the variable friction coefficient on 6111 aluminum alloy. Metals (Basel) 10(9):1189. https://doi.org/10.3390/met10091189

3. Trzepieciński T, Lemu HG (2014) "Frictional conditions of AA5251 aluminium alloy sheets using drawbead simulator tests and numerical methods. Strojniški Vestn–J Mech Eng 60(1):51–60. https://doi.org/10.5545/sv-jme.2013.1310

4. Sigvant M et al (2019) Friction in sheet metal forming: influence of surface roughness and strain rate on sheet metal forming simulation results. Procedia Manuf 29:512–519. https://doi.org/10.1016/j.promfg.2019.02.169

5. Zabala A et al (2021) The interaction between the sheet/tool surface texture and the friction/galling behaviour on aluminium deep drawing operations. Metals (Basel) 11(6):979. https://doi.org/10.3390/met11060979

6. Hol J, Wiebenga JH, Carleer B (2017) Friction and lubrication modelling in sheet metal forming: Influence of lubrication amount, tool roughness and sheet coating on product quality. J Phys Conf Ser 896:012026. https://doi.org/10.1088/1742-6596/896/1/012026

7. Sigvant M et al (2018) Friction in sheet metal forming simulations: modelling of new sheet metal coatings and lubricants. IOP Conf Ser Mater Sci Eng 418:012093. https://doi.org/10.1088/1757-899X/418/1/012093

8. Podulka P (2021) The effect of surface topography feature size density and distribution on the results of a data processing and parameters calculation with a comparison of regular methods. Materials (Basel) 14(15):4077. https://doi.org/10.3390/ma14154077

9. Trzepieciński T, Gelgele HL (2011) Investigation of anisotropy problems in sheet metal forming using finite element method. Int J Mater Form 4(4):357–369. https://doi.org/10.1007/s12289-010-0994-7

10. Trzepieciński T (2010) 3D elasto-plastic FEM analysis of the sheet drawing of anisotropic steel sheet. Arch Civ Mech Eng 10(4):95–106. https://doi.org/10.1016/S1644-9665(12)60035-1

11. Uyanık GK, Güler N (2013) A study on multiple linear regression analysis. Procedia - Soc Behav Sci 106:234–240. https://doi.org/10.1016/j.sbspro.2013.12.027

12. Tanaka H, Lee H (1998) Interval regression analysis by quadratic programming approach. IEEE Trans Fuzzy Syst 6(4):473–481. https://doi.org/10.1109/91.728436

13. Daoud JI (2017) Multicollinearity and regression analysis. J Phys Conf Ser 949:012009. https://doi.org/10.1088/1742-6596/949/1/012009

14. Kanyongo GY, Certo J, Launcelot BI (2006) Using regression analysis to establish the relationship between home environment and reading achievement: a case of Zimbabwe. Int Educ J 7(5):632–641

15. Matuszak A (2000) Factors influencing friction in steel sheet forming. J Mater Process Technol 106(1–3):250–253. https://doi.org/10.1016/S0924-0136(00)00625-7

16. Matuszak A, Gładysz K (2001) Definiowanie warunków tarcia podczas symulacji komputerowej procesów tłoczenia blach. Przegląd Mech 60:31–35

17. Dasgupta R, Thakur R, Govindrajan B (2002) Regression analysis of factors affecting high stress abrasive wear behavior. Pract Fail Anal 2(2):65–68. https://doi.org/10.1007/BF02715422

18. Jurkovic M, Jurkovic Z, Buljan S (2006) The tribological state test in metal forming processes using experiment and modelling,. J Achiev Mater Manuf Eng 18(1–2):383–386. [Online]. Available: http://ww.journalamme.org/papers_amme06/1152.pdf. Accessed 7 Aug 2022

19. Keum YT, Kim JH, Ghoo BY (2001) Expert drawbead models for finite element analysis of sheet metal forming processes. Int J Solids Struct 38(30–31):5335–5353. https://doi.org/10.1016/S0020-7683(00)00342-5

20. Aleksendrić D (2010) Neural network prediction of brake friction materials wear. Wear 268(1–2):117–125. https://doi.org/10.1016/j.wear.2009.07.006

21. Ibrahim D (2016) An overview of soft computing. Procedia Comput Sci 102:34–38. https://doi.org/10.1016/j.procs.2016.09.366

22. Kartam N (1997) Artificial neural networks for civil engineers: fundamentals and applications | semantic scholar. https://www.semanticscholar.org/paper/Artificial-Neural-Networks-for-Civil-Engineers:-and-Kartam-Flood/4a1113147a3b98b2717db9382a7143d435595d1a

23. Grymek S, Druet K, Łubiński J (2002) Perspektywy obliczeń neuronowych w inżynierii łożyskowania. Tribologia 33(1(181)):227–237

24. Aleksendrić D, Barton DC (2009) Neural network prediction of disc brake performance. Tribol Int 42(7):1074–1080. https://doi.org/10.1016/j.triboint.2009.03.005

25. Bao J, Minming T, Zhu Z, Yin Y (2012) Intelligent tribological forecasting model and system for disc brake. 2012 24th Chin Cont Decision Conf (CCDC) 3870–3874. https://doi.org/10.1109/CCDC.2012.6243100

26. Shebani A, Iwnicki S (2018) Prediction of wheel and rail wear under different contact conditions using artificial neural networks. Wear 406–407:173–184. https://doi.org/10.1016/j.wear.2018.01.007

27. Kurra S, Hifzur Rahman N, Regalla SP, Gupta AK (2015) Modeling and optimization of surface roughness in single point incremental forming process. J Mater Res Technol 4(3):304–313. https://doi.org/10.1016/j.jmrt.2015.01.003

28. Najm SM, Paniti I, Trzepieciński T, Nama SA, Viharos ZJ, Jacso A (2021) Parametric effects of single point incremental forming on hardness of AA1100 aluminium alloy sheets. Materials (Basel) 14(23):7263. https://doi.org/10.3390/ma14237263

29. Najm SM, Paniti I (2021) Predict the effects of forming tool characteristics on surface roughness of aluminum foil components formed by SPIF using ANN and SVR. Int J Precis Eng Manuf 22(1):13–26. https://doi.org/10.1007/s12541-020-00434-5

30. Najm SM, Paniti I (2021) Artificial neural network for modeling and investigating the effects of forming tool characteristics on the accuracy and formability of thin aluminum alloy blanks when using SPIF. Int J Adv Manuf Technol 114(9–10):2591–2615. https://doi.org/10.1007/s00170-021-06712-4

31. Trzepieciński T, LemuGelgele H (2012) Application of genetic algorithm for optimization of neural networks for selected tribological test. Acta Mech Slovaca 16(2):54–60. https://doi.org/10.21496/ams.2012.019

32. Quiza R, Figueira L, Paulo Davim J (2008) Comparing statistical models and artificial neural networks on predicting the tool wear in hard machining D2 AISI steel. Int J Adv Manuf Technol 37(7–8):641–648. https://doi.org/10.1007/s00170-007-0999-7

33. Rapetto MP, Almqvist A, Larsson R, Lugt PM (2009) On the influence of surface roughness on real area of contact in normal, dry, friction free, rough contact by using a neural network. Wear 266(5–6):592–595. https://doi.org/10.1016/j.wear.2008.04.059

34. Frangu L, Rîpă M (2001) Artificial neural networks applications in tribology – a survey. https://www.semanticscholar.org/paper/Artificial-Neural-Networks-Applications-in-%E2%80%93-A-Frangu-R%C3%AEp%C4%83/26585c4bc8e40a48b52fc09af0f6c0545cf781f7

35. Trzos M (2007) Tendencje rozwojowe w modelowaniu zjawisk i procesów tribologicznych. Zagadnienia Eksploat Masz 151(3):73–88

36. Yin N, Xing Z, He K, Zhang Z (2023) Tribo-informatics approaches in tribology research: A review. Friction 11(1):1–22. https://doi.org/10.1007/s40544-022-0596-7

37. Bhaumik S, Pathak SD, Dey S, Datta S (2019) Artificial intelligence based design of multiple friction modifiers dispersed castor oil and evaluating its tribological properties. Tribol Int 140:105813. https://doi.org/10.1016/j.triboint.2019.06.006

38. Pantić M et al (2018) Application of artificial neural network in biotribological research of dental glass ceramic. Tribol Ind 40(4):692–701. https://doi.org/10.24874/ti.2018.40.04.15

39. Gyurova LA, Friedrich K (2011) Artificial neural networks for predicting sliding friction and wear properties of polyphenylene sulfide composites. Tribol Int 44(5):603–609. https://doi.org/10.1016/j.triboint.2010.12.011

40. Bhaumik S, Kamaraj M (2021) Artificial neural network and multi-criterion decision making approach of designing a blend of biodegradable lubricants and investigating its tribological properties. Proc Inst Mech Eng Part J J Eng Tribol 235(8):1575–1589. https://doi.org/10.1177/1350650120965754

41. Nasir T, Yousif BF, McWilliam S, Salih ND, Hui LT (2010) An artificial neural network for prediction of the friction coefficient of multi-layer polymeric composites in three different orientations. Proc Inst Mech Eng Part C J Mech Eng Sci 224(2):419–429. https://doi.org/10.1243/09544062JMES1677

42. Echávarri Otero J et al (2014) Artificial neural network approach to predict the lubricated friction coefficient. Lubr Sci 26(3):141–162. https://doi.org/10.1002/ls.1238

43. Rosenkranz A, Marian M, Profito FJ, Aragon N, Shah R (2020) The use of artificial intelligence in tribology—a perspective. Lubricants 9(1):2. https://doi.org/10.3390/lubricants9010002

44. Marian M, Tremmel S (2021) Current trends and applications of machine learning in tribology—a review. Lubricants 9(9):86. https://doi.org/10.3390/lubricants9090086

45. Argatov I (2019) Artificial Neural Networks (ANNs) as a novel modeling technique in tribology. Front Mech Eng 5:30

46. Senkara L, Bobulska W, Alfa WN (1987) Blachy i taśmy stalowe dla przemysłu motoryzacyjnego PN-87/H-92143. Wydawnictwa Normalizacyjne ALFA

47. EN 10130 (2009) Cold rolled low carbon steel flat products for cold forming - technical delivery conditions. European Committee for Standardization Geneva

48. Trzepieciński T (2020) Tribological performance of environmentally friendly bio-degradable lubricants based on a combination of boric acid and bio-based oils. Materials (Basel) 13(17):3892. https://doi.org/10.3390/ma13173892

49. Szpunar M, Trzepieciński T, Żaba K, Ostrowski R, Zwolak M (2021) Effect of lubricant type on the friction behaviours and surface topography in metal forming of Ti-6Al-4V titanium alloy sheets. Materials (Basel) 14(13):3721. https://doi.org/10.3390/ma14133721

50. Trzepieciński T, Fejkiel R (2017) On the influence of deformation of deep drawing quality steel sheet on surface topography and friction. Tribol Int 115:78–88. https://doi.org/10.1016/j.triboint.2017.05.007

51. Prokhorenkova L, Gusev G, Vorobev A, Dorogush AV, Gulin A (2018) Catboost: unbiased boosting with categorical features. Adv Neural Inf Process Syst 2018(Section 4):6638–6648

52. Dorogush AV, Ershov V, Gulin A (2018) CatBoost: gradient boosting with categorical features support. 1–7 [Online]. Available: http://arxiv.org/abs/1810.11363. Accessed 7 Aug 2022

53. Ibragimov B (2019) Minimal variance sampling in stochastic gradient boosting. arXiv.org. https://arxiv.org/abs/1910.13204v1. Accessed 7 Aug 2022

54. Nabipour M, Keshavarz P (2017) Modeling surface tension of pure refrigerants using feed-forward back-propagation neural networks. Int J Refrig 75:217–227. https://doi.org/10.1016/j.ijrefrig.2016.12.011

55. Beale MH, Hagan MT, Demuth HB (2013) Neural Network Toolbox TM user ' s guide R2013b. MathworksInc

56. Riedmiller PM "Machine learning : multi layer perceptrons," Albert-Ludwigs-University Freibg. AG Maschinelles Lernen [Online]. Available: http://ml.informatik.uni-freiburg.de/_media/documents/teaching/ss09/ml/mlps.pdf. Accessed 7 Aug 2022

57. Principe J, Euliano NR, Lefebvre WC (1997) Neural and adaptive systems: fundamentals through simulation: multilayer perceptrons. Neural Adapt Syst Fundam Through Simulation© 1–108.https://doi.org/10.1002/ejoc.201200111.

58. Beale MH, Hagan MT, Demuth HB (2020) Deep learning toolbox TM user 's guide how to contact MathWorks. chrome-extension://efaidnbmnnnibpcajpcglclefindmkaj/https://ge0mlib.com/papers/Books/04_Deep_Learning_Toolbox_Users_Guide.pdf

59. Zhang G, Eddy Patuwo B, Hu MY (1998) Forecasting with artificial neural networks:: the state of the art. Int J Forecast

14(1):35–62. [Online]. Available: https://econpapers.repec.org/RePEc:eee:intfor:v:14:y:1998:i:1:p:35-62. Accessed 7 Aug 2022

60. Shahin M, Maier HR, Jaksa MB (2000) Evolutionary data division methods for developing artificial neural network models in geotechnical engineering Evolutionary data division methods for developing artificial neural network models in geotechnical engineering by M A Shahin M B Jaksa Departmen. https://hdl.handle.net/2440/33462. Accessed 7 Aug 2022

61. Lundberg SM, Lee S-I (2017) A unified approach to interpreting model predictions. Adv Neural Inform Process Syst 30 [Online]. Available: https://proceedings.neurips.cc/paper/2017/file/8a20a8621978632d76c43dfd28b67767-Paper.pdf. Accessed 7 Aug 2022

62. Štrumbelj E, Kononenko I (2014) Explaining prediction models and individual predictions with feature contributions. Knowl Inf Syst 41(3):647–665. https://doi.org/10.1007/s10115-013-0679-x

63. Bach S, Binder A, Montavon G, Klauschen F, Müller K-R, Samek W (2015) On pixel-wise explanations for non-linear classifier decisions by layer-wise relevance propagation. PLoS ONE 10(7):e0130140. https://doi.org/10.1371/journal.pone.0130140

64. Ribeiro MT, Singh S, Guestrin C (2016) "Why should i trust you?", Proc 22nd ACM SIGKDD Int Conf Knowledge Discov Data Mining 1135–1144. https://doi.org/10.1145/2939672.2939778.

65. Vatankhah E, Semnani D, Prabhakaran MP, Tadayon M, Razavi S, Ramakrishna S (2014) Artificial neural network for modeling the elastic modulus of electrospun polycaprolactone/gelatin scaffolds. Acta Biomater 10(2):709–721. https://doi.org/10.1016/j.actbio.2013.09.015

66. Rezakazemi M, Razavi S, Mohammadi T, Nazari AG (2011) Simulation and determination of optimum conditions of pervaporative dehydration of isopropanol process using synthesized PVA–APTEOS/TEOS nanocomposite membranes by means of expert systems. J Memb Sci 379(1–2):224–232. https://doi.org/10.1016/j.memsci.2011.05.070

67. Garson GD (1991) Interpreting neural-network connection weights. AI Expert 6(4):46–51

68. Ibrahim OM (2013) A comparison of methods for assessing the relative importance of input variables in artificial neural networks. J Appl Sci Res 9(11):5692–5700

69. Olden JD, Jackson DA (2002) Illuminating the 'black box': a randomization approach for understanding variable contributions in artificial neural networks. Ecol Modell 154(1–2):135–150. https://doi.org/10.1016/S0304-3800(02)00064-9